

U.S. DEPARTMENT OF INTERIOR
GEOLOGICAL SURVEY



North Atlantic Slope and Canyon Study

Volume 1

Executive Summary

by

Bradford Butman¹

Open-File Report 88-27A

Prepared in cooperation with
U.S. Minerals Management Service
IA14-12-001-30180

This report is preliminary and has not been reviewed for conformity with U.S. Geological Survey or Minerals Management Service editorial standards.

¹Woods Hole, MA 02543

U.S. DEPARTMENT OF INTERIOR
GEOLOGICAL SURVEY

NORTH ATLANTIC SLOPE AND CANYON STUDY

VOLUME 1

EXECUTIVE SUMMARY

by

Bradford Butman

Open-File Report 88-27A

Final report to
U.S. MINERALS MANAGEMENT SERVICE
Atlantic Outer Continental Shelf Regional Office
under Interagency Agreement
IA14-12-0001-30180

This report has been reviewed by the U.S. Minerals Management Service (MMS) and approved for publication. Approval does not signify that the contents necessarily reflect the views and policies of the MMS, nor does mention of trade names or commercial products constitute endorsement or recommendation for use by the U.S. Geological Survey (USGS) or the MMS. This report is preliminary and has not been reviewed for conformity with USGS editorial standards.

1988

Office of Energy and Marine Geology
Branch of Atlantic Marine Geology
Woods Hole, MA 02543

REPORT DOCUMENTATION PAGE	1. REPORT NO. MMS 86-0086	2.	3. Recipient's Accession No.
4. Title and Subtitle North Atlantic Slope and Canyon Study		5. Report Date December 1986	
7. Author(s) Edited by B. Butman. Authors: B. Butman, M.H. Bothner, V.D. Lyne, J.A. Moody, M.A. Noble, C.M. Parmenter, R.R. Rendigs		6.	
9. Performing Organization Name and Address and M. Rubin U.S. Geological Survey Branch of Atlantic Marine Geology Quissett Campus Woods Hole, MA 02543		8. Performing Organization Rept. No.	
12. Sponsoring Organization Name and Address U.S. Department of Interior Minerals Management Service Atlantic OCS 1951 Kidwell Drive, Vienna, VA 22180		10. Project/Task/Work Unit No.	
5. Supplementary Notes A two volume set: Vol. 1 Executive Summary, Vol. 2 Final Report		11. Contract(C) or Grant(G) No. (C) Interagency Agreement (G) IA 14-12-0001-30180	
6. Abstract (Limit: 200 words) A field program to investigate the currents and sediment transport along the outer-shelf and upper slope along the southern flank of Georges Bank was conducted between 1980 and 1984. A major part of the field experiment was conducted in Lydonia Canyon, a large submarine canyon which cuts northward about 20 km into the continental shelf from the shelfbreak. A smaller experiment was conducted in Oceanographer Canyon to compare the currents in these two major canyons. Long-term current observations were made at 20 locations in or adjacent to Lydonia Canyon, and at 9 stations on the continental slope. Detailed semi-synoptic hydrographic observations were made on 9 cruises. The long-term current observations made in Lydonia and Oceanographer Canyons show that the current regime in these topographic features differs from the adjacent slope, and between canyons. Based on the sediments, geochemistry, and currents observed in Lydonia Canyon, fine-grained sediments, some derived from the shelf, are accumulating in the head of the canyon. The canyons are not tranquil depositional environments however; sediments near the head (depths shallower than about 600 m) in both Lydonia and Oceanographer are frequently resuspended. This frequent resuspension may allow the sediments to strip pollutants from the water column. Currents in Oceanographer Canyon are stronger and the sediments coarser than in Lydonia at comparable depths. The currents associated with Gulf Stream warm core rings (WCR's) strongly affect the flow along the outer shelf and upper slope; eastward currents in excess of 75cm/s were associated with WCR's.		13. Type of Report & Period Covered Final Report 1984-1986	
7. Document Analysis a. Descriptors Lydonia Canyon, continental slope, Oceanographer Canyon, Georges Bank, North Atlantic, sediment transport, Gulf Stream warm core rings.		14.	
b. Identifiers/Open-Ended Terms			
c. COSATI Field/Group			
Availability Statement: Availability unlimited		19. Security Class (This Report) unclassified	21. No. of Pages V1 65; V2 563
		20. Security Class (This Page) unclassified	22. Price

VOLUME 1

TABLE OF CONTENTS

EXECUTIVE SUMMARY

	Page
Introduction.....	1
Field Program.....	4
Lydonia Canyon Experiment.....	4
Slope Experiment.....	15
Results.....	15
Canyon geometry and sediment texture.....	15
Currents.....	22
Suspended particle distribution.....	26
Sediment transport.....	32
Canyon comparisons.....	33
Currents over the slope.....	34
Instrument calibrations.....	34
Major Findings.....	35
Acknowledgements.....	37
References.....	38

VOLUME 2

TABLE OF CONTENTS

CHAPTER 1: INTRODUCTION

CHAPTER 2: AN OVERVIEW OF THE LYDONIA CANYON EXPERIMENT: SEDIMENTS,
HYDROGRAPHY, AND CURRENTS, by B. Butman

	Page
Abstract.....	2-1
Introduction.....	2-3
Field Program.....	2-6
Instrumentation.....	2-6
Moored array.....	2-8
Deployment 1.....	2-9
Deployments 2-5.....	2-13
Data Recovery.....	2-13
Mooring Position.....	2-24
Hydrography.....	2-25
Sediments.....	2-25
Results.....	2-28
Canyon topography.....	2-28
Surficial sediment texture.....	2-32
Hydrography.....	2-42
January 1981.....	2-43
May 1981.....	2-50
September 1981.....	2-50
February 1982.....	2-58
Summary of hydrography and suspended sediments.....	2-65
Currents.....	2-66
Spectra.....	2-66
Internal wave characteristics.....	2-87
Coherence structure in internal wave band.....	2-92
M ₂ tidal currents.....	2-94
Time variability of semidiurnal fluctuations.....	2-98
Mean flow.....	2-104
Deployment 1.....	2-105
Deployment 2-5.....	2-113
Relationship of mean flow to high-frequency fluctuations.....	2-116
Summary and discussion of mean flow.....	2-118
Gulf Stream Warm Core Rings.....	2-122
Frequency.....	2-122
Effects on shelf and canyon.....	2-124
Effect on near-bottom speeds.....	2-128
Currents near the bottom and sediment transport.....	2-132
Effect of storms.....	2-142
Oceanographer Canyon.....	2-145
Discussion.....	2-146
Acknowledgements.....	2-155
References.....	2-156

CHAPTER 3: SAND TRANSPORT AND FINE PARTICLE SUSPENSION WITHIN AND
AROUND LYDONIA CANYON, by V. D. Lyne and B. Butman

	Page
Abstract.....	3-1
Introduction.....	3-2
Field data.....	3-4
Mooring information.....	3-4
Bottom roughness observations.....	3-6
Wave and current measurements.....	3-14
Beam transmissometer fouling.....	3-15
Sediment transport model.....	3-17
Model application.....	3-23
Comparisons of measured and model attenuation.....	3-25
Predicted sand transport rates.....	3-31
Fine sediment transport.....	3-41
Relation to hydrography.....	3-43
Attenuation time-series interpretation.....	3-46
Vertical and horizontal interrelationships.....	3-46
Internal wave packets and sediment suspension.....	3-53
Discussion on internal wave effects.....	3-62
Conclusions.....	3-66
Acknowledgements.....	3-68
References.....	3-69

CHAPTER 4: MIXING OF WATER IN SUBMARINE CANYONS INDICATED BY CHANGES
IN TEMPERATURE-SALINITY CURVES, by J. A. Moody and B. Butman

	Page
Abstract.....	4-1
Introduction.....	4-1
Water masses.....	4-3
Georges Bank water.....	4-4
Scotian Shelf water.....	4-4
Winter water.....	4-6
Western North Atlantic water.....	4-6
Methods.....	4-8
Field measurements.....	4-8
Reference TS curve.....	4-8
Mixing types.....	4-10
Results.....	4-21
January 1981 (OCEANUS Cruise 91).....	4-21
April 1981 (OCEANUS Cruise 95).....	4-23
October 1981 (OCEANUS Cruise 104).....	4-23
January 1982 (OCEANUS Cruise 113).....	4-26
November 1982 (OCEANUS Cruise 130).....	4-26
Mixing time scales.....	4-26
Other canyons (OCEANUS Cruise 130).....	4-30
Summary.....	4-32
References.....	4-35

CHAPTER 5: THE REGIONAL STRUCTURE OF SUBTIDAL CURRENTS WITHIN AND AROUND LYDONIA CANYON, by M. A. Noble

	Page
Abstract.....	5-1
Introduction.....	5-2
Data Set.....	5-4
Results.....	5-12
The regional structure in the subtidal current field.....	5-12
Subtidal currents over the shelf.....	5-12
Subtidal currents over the slope.....	5-19
Subtidal currents in Lydonia Canyon.....	5-28
Coupling among the regional current fields.....	5-36
Wind-driven currents.....	5-40
Discussion.....	5-46
Summary.....	5-53
Acknowledgments.....	5-55
References.....	5-56

CHAPTER 6: THE FLUX AND COMPOSITION OF RESUSPENDED SEDIMENT IN SUBMARINE CANYONS OFF THE NORTHEASTERN UNITED STATES: IMPLICATIONS FOR POLLUTANT SCAVANGING, by M. H. Bothner, C. M. Parmenter, R. R. Rendigs, and M. Rubin

	Page
Abstract.....	6-1
Introduction.....	6-2
Equipment and methods.....	6-3
Sediment traps.....	6-3
Poison dispensers.....	6-6
Deployment and recovery.....	6-8
Laboratory methods.....	6-8
Results and Discussion.....	6-10
Comparison of different size traps.....	6-10
Sediment flux in different physiographic areas.....	6-11
Depth profile of resuspended sediment flux.....	6-19
Time variability in flux.....	6-19
Trace-metal concentrations in sediment-trap samples.....	6-30
Sediment sources.....	6-42
Potential of pollutant adsorption by resuspended sediments.....	6-48
Conclusions.....	6-55
References.....	6-57

CHAPTER 7: DOWNSLOPE FLOW ASSOCIATED WITH HIGH-FREQUENCY CURRENT
 FLUCTUATIONS OBSERVED ON THE OUTER CONTINENTAL SHELF
 AND UPPER-SLOPE ALONG THE NORTHEASTERN U.S. CONTINENTAL
 MARGIN: IMPLICATIONS FOR SEDIMENT TRANSPORT, by B. Butman

	Page
Abstract.....	7-1
Introduction.....	7-1
Field Program.....	7-3
Results.....	7-9
Hydrographic Setting.....	7-9
Mean Flow.....	7-16
Currents at Station SF.....	7-21
Near-bottom flow at other stations.....	7-37
Discussion and Conclusions.....	7-47
Acknowledgements.....	7-50
References.....	7-51

APPENDIX 1: A FIELD COMPARISON OF FOUR SEDIMENT TRAPS: CHANGES
 IN COLLECTION WITH TRAP GEOMETRY AND SIZE,
 by M. H. Bothner, B. Butman, and C. M. Parmenter

	Page
Abstract.....	A1-1
Introduction.....	A1-1
Equipment and Methods.....	A1-3
Traps.....	A1-3
Poison Dispensers.....	A1-5
Baffles.....	A1-6
Deployment and Recovery.....	A1-7
Current Measurements.....	A1-10
Laboratory Methods.....	A1-10
Results and Discussion.....	A1-11
Changes in collection rate with trap type.....	A1-11
Influence of mooring tilt.....	A1-17
Influence of poison.....	A1-18
Conclusions.....	A1-19
Acknowledgements.....	A1-20
References.....	A1-21

APPENDIX 2: NEAR-BOTTOM SUSPENDED MATTER CONCENTRATION ON THE
 CONTINENTAL SHELF DURING STORMS: ESTIMATES BASED
 ON IN-SITU OBSERVATIONS OF LIGHT TRANSMISSION AND A
 PARTICLE SIZE DEPENDENT TRANSMISSION CALIBRATION,
 by J. A. Moody and B. Butman

	Page
Abstract.....	A2-1
Introduction.....	A2-1
Theory.....	A2-4
Calibration Methods and Results.....	A2-5
Single particle classes.....	A2-5

	Page
Mixture of particle sizes.....	A2-11
Field Measurements.....	A2-14
Size distribution of trapped sediments.....	A2-22
Estimates of B and suspended-matter concentration.....	A2-25
Discussion.....	A2-30
Summary.....	A2-35
Acknowledgements.....	A2-36
References.....	A2-37

Volume 1

List of Illustrations

Figure		Page
1	Base map showing location of Lydonia Canyon.....	2
2a	Location of all moorings deployed as part of the Lydonia Canyon Experiment.....	6
2b	Location of moorings in and around Lydonia canyon.....	7
3	Base map and cross-section of Lydonia Canyon.....	8
4	Cruise track for OCEANUS 91.....	10
5a	Schematic of typical moorings deployed on the shelf as part of the Lydonia Canyon Experiment.....	11
5b	Schematic of typical moorings deployed in Lydonia Canyon and on the continental slope.....	12
6	Bottom tripod system.....	13
7	Deep instrument package.....	14
8	Location of moorings deployed as part of the Slope Array Experiment.....	16
9	Cruise track for OCEANUS 140.....	17
10	Bathymetric map of Lydonia Canyon.....	18
11	Percent silt plus clay in the surficial sediments on the southern flank of Georges Bank near Lydonia and Oceanographer Canyons.....	20
12	Surficial sediment texture along the axis of Lydonia Canyon.....	21
13a	Schematic of the Eulerian mean flow on the shelf and slope adjacent to Lydonia Canyon.....	23
13b	Schematic of the upcanyon-downcanyon Eulerian mean flow along the axis of Lydonia Canyon.....	25
14	Histogram of near-bottom currents along the axis of Lydonia and Oceanographer Canyons.....	27
15	Hydrographic section along the axis of Lydonia canyon made in January 1981.....	28

Figure		Page
16	Histogram of the current of sediment caught in traps of different heights above the bottom.....	29
17	Time series of currents at LCB.....	30
18	Bottom photograph at LCB.....	31

Volume 1

List of Tables

Table		Page
1	Dates of moored array and hydrographic cruises conducted as part of the Lydonia Canyon and Slope Experiment.....	5

Volume 2

List of Illustrations

Figure		Page
2-1	Base map showing location of Lydonia Canyon on the southern flank of Georges Bank.....	2-4
2-2	Map of Lydonia Canyon and section along the canyon axis showing location of instruments in D1.....	2-10
2-3	Map of Lydonia Canyon and section along the canyon axis showing locaton of instruments in D2.....	2-14
2-4	Map of Lydonia Canyon and section along the canyon axis showing location of instruments in D3.....	2-16
2-5	Map of Lydonia Canyon and section along the canyon axis showing location of instruments in D4.....	2-18
2-6	Map of Lydonia Canyon and section along the canyon axis showing location of instruments in D5.....	2-20
2-7	Time line of all current measurements made as part of the Lydonia Canyon Experiment.....	2-23
2-8a	Location of hydrographic sections for OCEANUS 91 and 95. Circled numbers indicate the section number.....	2-26
2-8b	Location of hydrographic sections for OCEANUS 104 and 117. Circled numbers indicate the section number.....	2-27
2-9	Detailed bathymetric map of Lydonia Canyon.....	2-29
2-10	Bottom slope along the axis of Lydonia Canyon.....	2-31
2-11	Bathymetric sections across the axis of Lydonia Canyon....	2-33
2-12a	Surface sediment texture on the southern flank of Georges Bank adjacent to Lydonia and Oceanographer Canyons. Mean phi.....	2-35
2-12b	Surface sediment texture on the southern flank of Georges Bank adjacent to Lydonia and Oceanographer Canyons. Percent silt plus clay.....	2-36
2-12c	Surface sediment texture on the southern flank of Georges Bank adjacent to Lydonia and Oceanographer Canyons. Percent very fine sand.....	2-37

Figure		Page
2-13a	Surface sediment texture across the southern flank of Georges Bank and along the thalweg of Lydonia Canyon to 1,600 m. Mean Φ	2-39
2-13b	Surface sediment texture across the southern flank of Georges Bank and along the thalweg of Lydonia Canyon to 1,600 m. Percent silt plus clay, sand, and gravel.....	2-40
2-13c	Surface sediment texture across the southern flank of Georges Bank and along the thalweg of Lydonia Canyon to 1,600 m. Percent coarse sand (0.5-1.0 mm), medium sand (0.250-0.500 mm), fine sand (0.125-0.250 mm), and very fine sand (0.063-0.125 mm).....	2-41
2-14a	Section 4 made on OCEANUS 91 showing temperature, salinity, sigma-t, and beam attenuation across the shelf and slope east of Lydonia Canyon.....	2-44
2-14b	Section 3 made on OCEANUS 91 showing temperature, salinity, sigma-t, and beam attenuation along the axis of Lydonia Canyon.....	2-45
2-14c	Section 2 made on OCEANUS 91 showing temperature and salinity across the mouth of Lydonia Canyon.....	2-47
2-14d	Section 2 made on OCEANUS 91, showing sigma-t and beam attenuation across the mouth of Lydonia Canyon.....	2-48
2-14e	Vertical distribution of suspended matter at selected stations.....	2-49
2-15a	Section 6 made on OCEANUS 95 showing temperature, salinity, and sigma-t, across the shelf and slope east of Lydonia Canyon.....	2-51
2-15b	Section 5 made on OCEANUS 95 showing temperature, salinity, and sigma-t along the axis of Lydonia Canyon....	2-52
2-16a	Section 5 made on OCEANUS 104 showing temperature, salinity, sigma-t, and beam attenuation across the shelf and slope east of Lydonia Canyon.....	2-54
2-16b	Section 7 made on OCEANUS 104 showing temperature, salinity, sigma-t, and beam attenuation and along the axis of Lydonia Canyon.....	2-55
2-16c	Vertical distribution of suspended matter at selected stations.....	2-56
2-16d	Vertical distribution of suspended matter at selected stations.....	2-57

Figure		Page
2-16e	Vertical distribution of suspended matter at selected stations.....	2-59
2-17a	Section 2 made on OCEANUS 113 showing temperature, salinity, sigma-t, and beam attenuation across the shelf and slope to the east of Lydonia Canyon.....	2-60
2-17b	Section 5 made on OCEANUS 113 showing temperature, salinity, sigma-t, and beam attenuation along the axis of Lydonia Canyon.	2-61
2-17c	Section 3 made on OCEANUS 113 showing temperature and salinity across the mouth of Lydonia Canyon.....	2-62
2-17d	Section 3 made on OCEANUS 113 showing sigma-t and beam attenuation across the mouth of Lydonia Canyon.	2-63
2-17e	Vertical distribution of suspended matter at selected stations.....	2-64
2-18	Variance conserving spectra of currents at LCA, LCI, LCB, LCE and LCH on the shelf, slope and in Lydonia Canyon.	2-74
2-19	Current ellipses in the low-frequency (LF), diurnal (D), inertial (I), semidiurnal (SD) and high-frequency (HF) band at LCB and LCI.....	2-80
2-20	Near-bottom current ellipses along the axis of Lydonia Canyon showing current ellipse orientaton, amplitude, and stability in five frequency bands.....	2-81
2-21a,b	Section along the axis of Lydonia Canyon showing the amplitude of the current fluctuations in the high-frequency, and semidiurnal band.....	2-83
2-21c,d	Section along the axis of Lydonia Canyon showing the amplitude of the current fluctuations in the inertial and low-frequency band.....	2-84
2-22	Brunt-Vaisaila frequency (in cycles/hour) along the axis of Lydonia Canyon.....	2-88
2-23	Amplitude of energy near the bottom along the axis of Lydonia Canyon by frequency band.....	2-91
2-24	Percent of energy in the M ₂ tidal band (periods 12.21 to 12.52 hours) which is coherent with the tide on the shelf.....	2-96

Figure		Page
2-25	Amplitude of the major axis of the tidal ellipse and phase of the coherent M_2 (periods 12.31 to 12.52 hours) current.....	2-97
2-26	Amplitude of the current at the M_2 tidal period determined in 128 hour segments for the long-term observations at LCB (100 m) and LCB (5 mab).....	2-99
2-27a	Time-series plot of hour-averaged up-canyon current at LCE at 6 mab and 106 mab, beam attenuation at 6 mab, and bottom pressure at LCA during D3.....	2-101
2-27b	Time-series plot of hour-averaged upcanyon current at LCB(248) and LCB(294), beam attenuation at LCB(294), current at LCS(5 mab) and bottom pressure at LCL during D4.....	2-102
2-27c	Time-series plot of hour-averaged current at LCU(7 mab), beam attenuation at LCU(7 mab), current at LCB(5 mab) and bottom pressure at LCA during D5.....	2-103
2-28	Weekly Ocean Frontal Analysis charts for November 1980 to February 1981. The locations of the moorings are shown as small dots.....	2-106
2-29a	Monthly mean Eulerian currents during D1 (November and December, 1980).....	2-107
2-29b	Monthly mean Eulerian currents during D1 (January and February, 1981).....	2-108
2-29c	Monthly mean Eulerian currents during D1 (March and April, 1981).....	2-109
2-30a	Mean Eulerian current for D1 and D2.....	2-111
2-30b	Mean Eulerian current for D3 and D4.....	2-114
2-30c	Mean Eulerian current for D5.....	2-117
2-31a	Preliminary schematic of the Eulerian mean flow on the and slope adjacent to Lydonia Canyon and along the walls of the canyon.....	2-119
2-31b	Preliminary schematic of Lydonia Canyon showing upcanyon-downcanyon component the mean Eulerian current at LCB, LCS, and LCE along the canyon axis.....	2-121
2-32	Low-passed along-slope component of flow at LCI(55) and LCI(5 mab) for D1 through D4.....	2-123
2-33	Vector stickplot of low-passed current at LCB(92), LCL(65), LCE(116), LCI(55) and LCJ(103) during D1.....	2-125

Figure		Page
2-34	Vector stickplot of low-passed current at LCB, LCQ, LCR, LCT and LCI during D4.....	2-127
2-35	Low-passed temperature at selected stations during D4.....	2-129
2-36	Schematic of flow induced by WCRs around the mouth of Lydonia Canyon at about 200 m based on observations made during WCR 82-A.....	2-130
2-37	Histogram of current speeds 5 mab at LCI during ring and non-ring periods.....	2-131
2-38	Cumulative speed distribution curve for stations along the canyon axis showing percent occurrence in excess of given speed.....	2-133
2-39a	Time series of temperature, beam attenuation, speed and upcanyon current at LCB1 (5 mab).....	2-135
2-39b	Time series of temperature, beam attenuation, speed and upcanyon current at LCB4 (5 mab).....	2-136
2-39c	Time series of temperature, beam attenuation, speed and upcanyon current at LCE1 (5 mab).....	2-137
2-39d	Time series of temperature, beam attenuation, speed and upcanyon current at LCU (5 mab).....	2-138
2-40	Scatterplot of hour-averaged currents at LCU, LCB, LCS, and LCE.....	2-140
2-41	Histogram of near-bottom currents greater than 30 cm/s and between 20 and 30 cm/s as a function of direction for stations along the axis of Lydonia Canyon.....	2-141
2-42	Standard deviation of bottom pressure at shelf stations during D1 through D5 indicating periods of major wave activity near the bottom.....	2-143
2-43	Histogram of near-bottom currents greater than 40 cm/s and between 30 and 40 cm/s at stations OCB and OCC in the axis of Oceanographer Canyon.....	2-147
2-44	Net Eulerian near-bottom flow in Oceanographer Canyon at OCB and OCC.....	2-148
2-45	Time series of observations made 6 mab at station OCC.....	2-149
3-1	Bottom photograph at station LCA.....	3-7
3-2	Bottom photograph at station LCM.....	3-8
3-3	Bottom photograph at station LCB.....	3-9

Figure		Page
3-4	Bottom photograph at station LCE.....	3-10
3-5	Bottom photograph near station LCS.....	3-11
3-6	Bottom photograph at station LCH.....	3-12
3-7	Bottom photograph at station LCI.....	3-13
3-8	Output from constrained digital filter.....	3-16
3-9	Measured and predicted attenuation at LCA.....	3-27
3-10	Measured and predicted attenuation at LCB.....	3-28
3-11	Measured and predicted attenuation at LCE.....	3-29
3-12	Measured and predicted attenuation at LCM.....	3-30
3-13a	Predicted sand transport roses for stations surrounding Lydonia Canyon.....	3-33
3-13b	Predicted sand transport roses for Lydonia Canyon axis stations.....	3-34
3-13c	Predicted percentage of time of sand transport for stations surrounding Lydonia Canyon.....	3-36
3-13d	Predicted percentage of time of sand transport for canyon axis stations.....	3-37
3-14	Vertical cross-section of salinity and beam attenuation coefficient.....	3-44
3-15a	Time-series of beam attenuation at LCA, LCB and LCE for measurements 20 mab or more.....	3-47
3-15b	Time-series of beam attenuation at LCB and LCE for measurements 5 mab.....	3-48
3-16	Measured and predicted attenuation at LCB.....	3-50
3-17	Measured and predicted attenuation at LCE.....	3-51
3-18a	Time-series of measurements at LCB during energetic internal wave activity.....	3-54
3-18b	Time-series of attenuation, speed shear and vertical temperature difference during energetic internal wave activity.....	3-55
3-19	Measured and predicted attenuation at LCB.....	3-59

Figure		Page
3-20	Comparison of hourly and 450 second current speed at LCB.....	3-20
3-21	Predicted attenuation at LCB using 450 second data.....	3-21
3-22	Semidiurnal packets of upcanyon speed and attenuation at LCB.....	3-22
4-1	Location of submarine canyons.....	4-2
4-2	Water mass characteristics.....	4-5
4-3	Standard Western North Atlantic TS curve.....	4-7
4-4	Hydrographic stations.....	4-9
4-5a	Western North Atlantic salinity anomaly versus depth.....	4-11
4-5b	Western North Atlantic salinity anomaly versus density....	4-12
4-5c	Western North Atlantic salinity anomaly for OCEANUS 95....	4-13
4-6	Hypothetical TS curves for internal mixing.....	4-15
4-7a	Vertical mixing of a local salinity minimum.....	4-16
4-7b	Vertical mixing of a local salinity maximum.....	4-17
4-7c	Vertical mixing resulting in a salinity increase and decrease at different depths.....	4-18
4-8a	External mixing with less saline water.....	4-19
4-8b	External mixing with a second water mass.....	4-20
4-9	January 1981 canyon salinity anomaly.....	4-22
4-10	April-May 1981 canyon salinity anomaly.....	4-24
4-11	September-October 1981 canyon salinity anomaly.....	4-25
4-12	January-February 1982 canyon salinity anomaly.....	4-27
4-13	November 1982 canyon salinity anomaly.....	4-28
4-14	Time series of Western North Atlantic salinity anomaly near Lydonia Canyon.....	4-29
4-15a	TS curves for Oceanographer Canyon.....	4-31
4-15b	TS curves for Welker Canyon.....	4-32

Figure		Page
5-1	Location of Lydonia Canyon and the Nantucket wind measurement site.....	5-3
5-2	Locations of the current-meter moorings deployed in and around Lydonia Canyon.....	5-7
5-3	Locations of the current meters within and above Lydonia Canyon showing the mooring name and current-meter category.....	5-8
5-4	Wind stress and typical current-meter records illustrating the flow on the shelf, slope and in the canyon.....	5-13
5-5	The first mode for alongshelf currents over the shelf.....	5-18
5-6	Coherence between mid-depth currents at shelf site LCL(70) and the first mode, Shelf EOF, currents.....	5-20
5-7	Variance-conserving spectra of alongshelf currents and wind stress and cross-shelf currents and wind stress.....	5-21
5-8	The first mode along-slope currents for Slope(200) EOF and Slope(500) EOF.....	5-24
5-9	Variance-conserving spectra of along-slope currents at Slope(200) and Slope(500) sites.....	5-25
5-10	Cross-slope current amplitudes at sites in the second Slope(200) EOF mode.....	5-27
5-11	Subtidal along-canyon current amplitudes at all canyon sites.....	5-31
5-12	Mean along-canyon current amplitudes at canyon sites.....	5-32
5-13	Variance-conserving spectra of along and cross-canyon currents.....	5-33
5-14	The amplitude of Mode 1 along-canyon currents.....	5-37
6-1	Map showing locations of moorings in and around Lydonia and Oceanographer Canyons.....	6-4
6-2	Diagram showing physical dimensions of sediment traps.....	6-5
6-3	Histograms showing the flux of resuspended sediments at different locations and depths in Lydonia Canyon.....	6-15
6-4	Comparison of sediment flux at different locations in the study area.....	6-17

Figure		Page
6-5	Comparison of sediment flux in Lydonia and Oceanographer Canyons.....	6-18
6-6	Flux of sediments in axis of Lydonia Canyon during 5 deployment periods.....	6-20
6-7	Sediment flux in the axis of Lydonia Canyon, station LCB..	6-22
6-8	Record of pressure standard deviation measured near the rim of Lydonia Canyon for each deployment period.....	6-23
6-9	Comparison of sediment flux in Lydonia Canyon axis and on the Continental Shelf at 5 meters above bottom.....	6-24
6-10	Diagram showing texture, structure, and x-radiograph of a sediment trap sample from station LCA. Calculated stress and predicted flux also shown.....	6-25
6-11	Diagram showing texture, structure, and x-radiograph of a sediment trap sample from station LCP. Calculated stress and predicted flux also shown.....	6-28
6-12	X-radiographs of trap samples from station LCB.....	6-31
6-13	Histograms showing the average metal to aluminum ratio in sediment trap samples from different geographical areas.....	6-38
6-14	Concentrations of barium in the fine fraction of sediment collected at station LCB during 5 deployments.....	6-44
6-15	¹⁴ C age of organic carbon in sediment cores from the head of Lydonia Canyon.....	6-47
7-1a	Bathymetric map showing location of current measurements made along the outer shelf and upper slope south of New England.....	7-4
7-1b	Detailed map showing location of moorings near 70°W.....	7-5
7-2	Hydrographic sections of temperature, salinity, sigma-t, Brunt-Vaisaila frequency, and beam attenuation made across the outer shelf and upper slope near 70°W.....	7-11
7-3	Near-bottom mean flow observed at selected stations during slope array II, slope array III, and the Lydonia Canyon experiment.....	7-18
7-4	Time series of temperature, speed, beam attenuation, and hour hour-averaged and low-passed along-slope and cross-slope current at station SF for record 2751 (126 m, 76 mab) and record 2752 (195 m, 7 mab).....	7-23

Figure		Page
7-5	Time series of beam attenuation, salinity, temperature, speed, and cross-slope current at 7 mab at station SF.....	7-26
7-6	Histogram of near-bottom current speed, and histogram of current direction for various speed intervals for currents measured at station SF at 7 and 76 mab.....	7-29
7-7	Variance conserving kinetic energy spectra for currents observed at station SF at 7 and 76 mab.....	7-30
7-8	Current ellipses at 7 and 76 mab at station SF for energy in the low frequency, diurnal, inertial, semidiurnal, and high frequency bands.....	7-31
7-9	Coherence between the along-slope and cross-slope currents at station SF at 7 and 76 mab.....	7-33
7-10	Coherence between the cross-slope current and sigma-t at 7 mab and 76 mab at station SF.....	7-36
7-11	Scatter plot of low-passed cross-slope Reynolds flux of density (sigma-t) vs low-passed cross-slope current at station SF.....	7-38
7-12	Time series plot of a portion of record 2752 at station SF illustrating the procedure used to estimate the envelope of the high frequency current fluctuations...	7-39
7-13	Scatter-plot of low-passed cross-slope flow vs amplitude of high-frequency fluctuations for currents at 7 and 76 mab at station SF.....	7-40
7-14	Speed exceeded 5% of the time, downslope flow exceeded 1% of the time, and ratio of down-slope flow exceeded 1% of the time to upslope flow exceeded 1% of the time for measurements at 7 and 50-200 mab as a function of water depth.....	7-41
7-15	Scatter plot of low-passed cross-slope flow vs amplitude of high frequency fluctuations for currents at 7 and 50-200 mab at LCI, SE, and SG in water depths of 250, 500, and 1150 m respectively.....	7-44
7-16	Net cross-slope flow vs standard deviation of cross-slope flow for current observations 5-7 mab at stations SF, LCI, SA, SE, and SG at nominal water depths of 200, 250, 500, and 1150 m.....	7-45
A1-1	Physical dimensions of the sediment traps used in this experiment.....	A1-4
A1-2	Configuration of the poison dispenser.....	A1-4

Figure		Page
A1-3	Map showing the station locations and a schematic showing trap spacing on the mooring wire.....	A1-9
A1-4	Variation in the flux of sediment for traps of different diameter.....	A1-12
A1-5	Variation in the flux of trapped sediment as a function of traps aspect ratio.....	A1-15
A2-1	Transmissometer calibration slope B_1 as function of particle diameter.....	A2-8
A2-2	Size distribution of tested sediment mixtures.....	A2-12
A2-3	Station locations.....	A2-14
A2-4	Bottom photographs.....	A2-15
A2-5	Time series for station K.....	A2-19
A2-6	Time series for station B.....	A2-20
A2-7	Graphic representation of an x-ray photograph of material collected in a sediment trap.....	A2-23

Volume 2

List of Tables

Table		Page
2-1	Dates of moored array deployments and hydrographic cruises.....	2-7
2-2	Mooring information for Deployment 1 of the moored array.....	2-11
2-3	Mooring information for Deployment 2 of the moored array.....	2-15
2-4	Mooring information for Deployment 3 of the moored array.....	2-17
2-5	Mooring information for Deployment 4 of the moored array.....	2-19
2-6	Mooring information for Deployment 5 of the moored array.....	2-21
2-7	Mooring information for moorings in Oceanographer Canyon.....	2-22
2-8a	Statistics of hour-averaged current observations.....	2-67
2-8b	Statistics of low-passed current observations.....	2-70
2-8c	Statistics of hour-averaged and low-passed current observations made in Oceanographer Canyon.....	2-73
2-9	Total energy and ellipse statistics by frequency band.....	2-76
2-10	Confidence limits for current amplitude.....	2-85
2-11	Bottom slope, range of Brunt-Vaisaila frequencies, and critical period for segments of the axis of Lydonia Canyon.....	2-90
2-12	Coherence and phase between selected current observations at the inertial, semi-diurnal and high-frequency periods.....	2-93
2-13	A comparison of current statistics in Lydonia, Oceanographer and Baltimore Canyons.....	2-153

Table		Page
3-1	Location and deployment information.....	3-5
3-2	Model parameters for bottom roughness and surficial sediment.....	3-24
3-3	Components of predicted net sand transport.....	3-32
5-1	Locations of current meters in and around Lydonia Canyon in Deployment 1.....	5-5
5-2	Ellipse statistics of the subtidal flow field.....	5-10
5-3	Mean and variance of the subtidal currents at each site.....	5-15
5-4	The first mode in the along and cross-shelf currents.....	5-17
5-5	The first mode in the along and cross-slope currents over the slope.....	5-22
5-6	Coherences among the slope(200) and slope(500) alongslope currents.....	5-29
5-7a	Correlations and coherences among the alongcanyon currents.....	5-34
5-7b	First mode for alongcanyon currents.....	5-35
5-8	Coherences among the regional currents.....	5-38
5-9	Correlation of the alongisobath shelf and slope modal currents with the alongcanyon currents.....	5-41
5-10a	Coherences between the alongshelf wind stress and alongisobath currents.....	5-43
5-10b	Coherences between cross-shelf wind stress and alongisobath currents.....	5-44
5-10c	Coherences between 110 ^o wind stress and alongisobath currents.....	5-45
5-11	Angle between the wind stress and alongisobath current that represents the maximum coherent current forcing.....	5-47
5-12	The coherence between alongisobath wind stress and cross-slope currents.....	5-48

Table		Page
6-1	Sediment-trap deployments and flux data.....	6-12
6-2A	Chemical analyses of sediment-trap samples before drilling.....	6-32
6-2B	Chemical analyses of sediment-trap samples-continued.....	6-33
6-2C	Chemical analyses of sediment-trap samples-continued.....	6-34
6-2D	Sediment-trap deployments-continued.....	6-35
6-2E	Sediment-trap locations and deployment dates-continued....	6-36
6-3	¹⁴ C ages determined on total organic carbon in sediment.....	6-46
6-4	Sediment radionuclide distributions.....	6-50
6-5	Textural analyses of box cores.....	6-53
7-1	Station identifier, water-depth, and location of stations where current observations were made.....	7-7
7-2	Statistics of the alongisobath and crossisobath currents.....	7-8
7-3	Total energy and ellipse statistics for currents in low-frequency, diurnal, inertial, semi-diurnal and high-frequency bands.....	7-32
A1-1	Deployment data and results of two sediment trap comparison experiments.....	A1-8
A1-2	Statistics of currents measured at station LCS and LCB.....	A1-14
A2-1	Calibration slopes B_i	A2-7
A2-2	Comparison of predicted and measured calibration slopes B	A2-11
A2-3	Estimates of suspended-matter concentration during six winter storms.....	A2-28
A2-4	Field measurements of the calibration slope \bar{B}	A2-31
A3-1	Lydonia Canyon Experiment; mooring locations and data quality.....	A3-2
A4-1	Slope Experiment; mooring locations and data quality.....	A4-2

EXECUTIVE SUMMARY

by

Bradford Butman

INTRODUCTION

Two major field experiments were conducted as part of the North Atlantic Slope and Canyon Study: the Lydonia Canyon Experiment and the Slope Experiment. These studies were initiated by the U.S. Minerals Management Service (MMS) and the U.S. Geological Survey (USGS) as interest in oil and gas exploration in the North Atlantic region moved offshore to the continental slope from the southern flank of Georges Bank. The major objectives of the field program were to provide a regional description of currents and sediment transport on the outer shelf and upper slope and within submarine canyons, and to understand the processes which cause sediment transport. A long-range goal of the program was to assess the long-term fate of material introduced into the water column or seafloor along the margin.

The continental slope is a relatively narrow transition region between the continental shelf and continental rise (fig. 1). Along the east coast of the United States, the texture of the surficial sediment changes from primarily sand to finer grained silt and clay just seaward of the shelf break, indicating a transition from an active sedimentary environment on the shelf to a more depositional environment on the upper slope. Because anthropogenic pollutants often are associated with fine-grained particles (Bothner and others, in press; Farrington and Boehm, in press; Morel and Schiff, 1983; Huggett and others, 1980) over long periods of time the slope may be a region of accumulation for these contaminants. Therefore, it is possible that particles introduced by exploratory drilling on the Outer Continental Shelf (OCS) may ultimately deposit on the continental slope.

The continental slope is dissected by major submarine canyons and numerous smaller gullies. Scanlon (1984) estimates that on the slope south of Georges Bank at depths shallower than 1500 m, as much as 80 percent of the

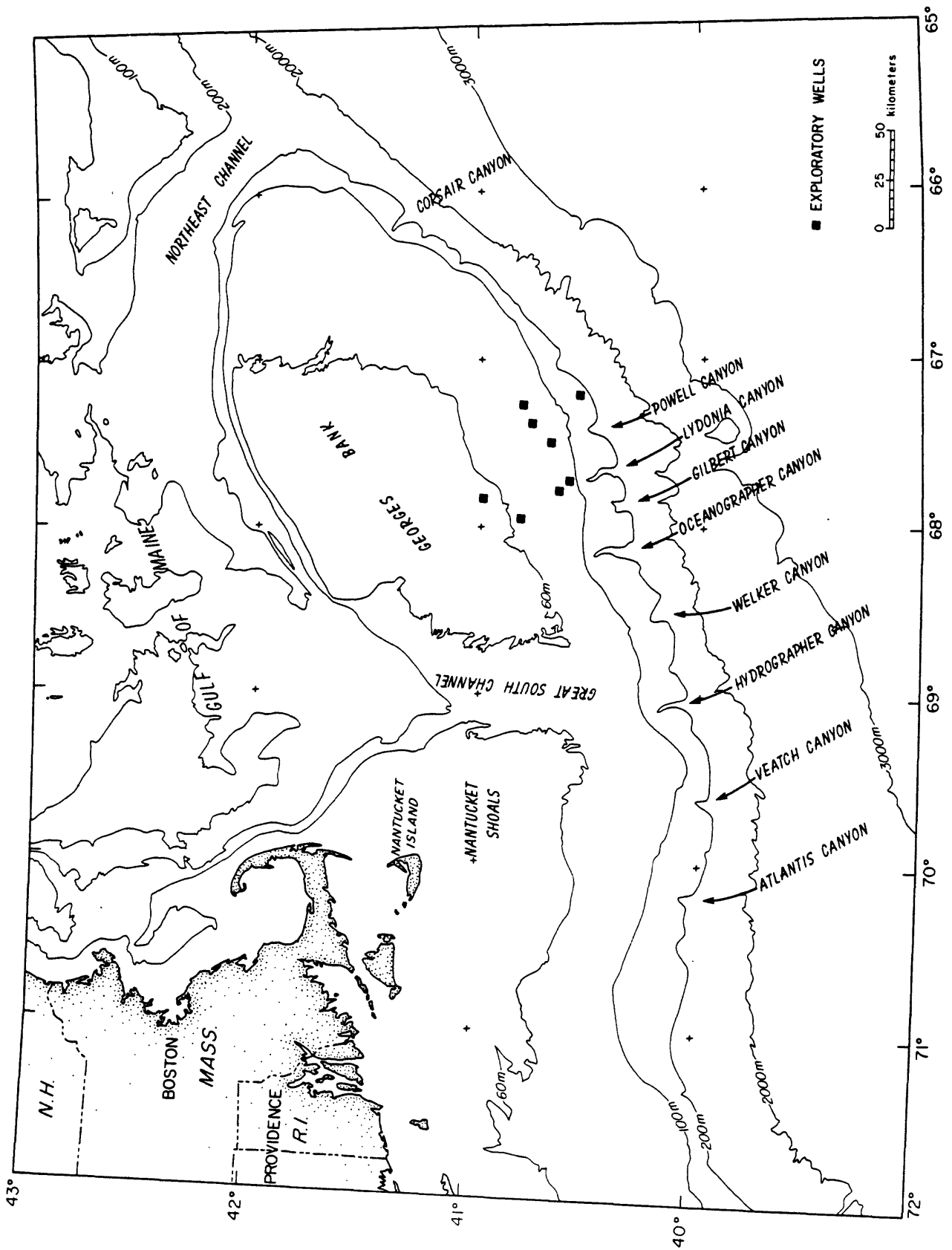


Figure 1. Base map showing location of Lydonia Canyon along the southern flank of Georges Bank. The continental shelf extends to the 200 m isobath, the continental slope from about the 200 m to 2000 m isobath, and the rise begins at depths of about 3000 m. Squares indicate the location of the eight exploratory wells drilled on Georges Bank.

slope is occupied by these canyons and gullies. The major canyons cut northward into the shelf as much as 20 km and may capture sediments from the shelf. The canyons may also provide a source of deep ocean water landward of the shelfbreak. The role of submarine canyons in the transport of sediment from the shelf to rise has long been of interest to marine geologists. The canyons also provide a variety of substrates for marine organisms and the diverse fauna have been the subject of several studies (Lamont Doherty Geological Observatory, 1983; Maciolek and others, 1986).

The circulation on the outer shelf and upper slope is a complex transition between the flow on the shelf and the flow in the deep ocean; a rich diversity of currents and processes of sediment transport is expected in this transition region. On the continental shelf, winter storms, tidal currents, and the westward residual mean flow are the primary factors which influence the net transport of sediment (Butman, in press). At the edge of the shelf, sediment movement may also be caused by internal waves, Gulf Stream warm core rings, and more complex flows associated with meanders of the Gulf Stream. Storms will be less important in deeper water because the wave currents, of major importance in resuspending sediments on the shelf, decrease rapidly with increasing water depth.

Several other recent field programs provide additional observations of currents on the outer continental margin. The Lydonia Canyon Experiment complements studies of Baltimore Canyon in the Middle Atlantic Bight (Lamont Doherty Geological Observatory, 1983) and of Quinault Canyon off the coast of Oregon (Carson and others, 1986). The Shelf Edge Exchange Processes (SEEP) study (Department of Energy) conducted along 70° W; and the Mid-Atlantic Slope and Rise study (MASARS) funded by MMS, provide observations to the west of those made as part of the Slope Experiment (Csanady and others, submitted).

Understanding the fate of pollutants and sediments introduced onto the shelf and slope, which is provided by these and other programs, is essential for sound management of the resources of the continental margin.

FIELD MEASUREMENTS

Lydonia Canyon Experiment

The Lydonia Canyon Experiment was conducted over a two-year period. The components of the program were: (1) detailed bathymetric surveys of the canyon and the adjacent shelf and slope; (2) surveys of the surficial sediment texture; (3) longterm measurements by an array of moored current meters, bottom tripods and sediment traps; (4) synoptic hydrographic observations; (5) bottom surveys utilizing sidescan sonographs and high resolution acoustic profiles; and (6) surveys of the canyon utilizing a research submersible. All of these field measurements were designed to describe the shelf and canyon environments and the transport of water and sediment within and between them. Lydonia Canyon was selected for study because it was closest to the exploratory drilling sites (fig. 1).

The moored array experiments were the largest component of the canyon experiment. Five deployments of instruments were made between November 1980 and November 1982 (table 1; fig. 2). The measurements were designed to document the flow within the canyon and near the bottom over the shelf and slope. Measurements were made throughout most of the experiment at LCA, LCB, LCE (or LCS), and LCI (fig. 2) to provide continuity between deployments and to assess long-term variability at typical shelf, canyon, and slope stations. In all of the moored array experiments, instruments were deployed on the shelf and slope and in the canyon at depths above and below the canyon rim (fig. 3). Limited observations were made at two stations in Oceanographer Canyon (fig. 1) to compare the current regimes of two major canyons.

Table 1. Dates of moored array deployments and hydrographic cruises conducted as part of the Lydonia Canyon Experiment and the Slope Experiment. Roman numerals indicate moored array deployments. Stations indicate the locations where moorings were deployed in each experiment (see fig. 2 and 8).

<u>Deployment</u>		<u>Date</u>	<u>Cruise</u>	<u>Stations</u>
<u>Start</u>	<u>Stop</u>			
<u>Lydonia Canyon Experiment</u>				
I		November 1980	OCEANUS 88	LCA, LCC, LCD, LCF, LCG, LCM
I		December 1980	OCEANUS 90	LCA, LCB, LCE, LCH, LCI, LCJ LCK, LCL, LCM, LCN
		January 1981	OCEANUS 91	LCO
II	I	April 1981	OCEANUS 95	LCA, LCB, LCE, LCI
III	II	September 1981	OCEANUS 104	LCA, LCB, LCE, LCI, LCO, LCP
IV	III	January 1982	OCEANUS 113	LCA, LCB, LCI, LCL, LCO, LCQ LCR, LCS, LCT, OCA, OCB, OCC
V	IV	July 1982	OCEANUS 122	LCA, LCB, LCU
	V	November 1982	OCEANUS 130	
<u>Slope Experiment</u>				
I		November 1982	OCEANUS 130	SA, SB, SC, SD, SE
II	I	October 1983	OCEANUS 140	SA, SE, SF
III	II	March 1984	OCEANUS 149	SA, SE, SF, SG, SH, T
	III	November 1984	OCEANUS 159	

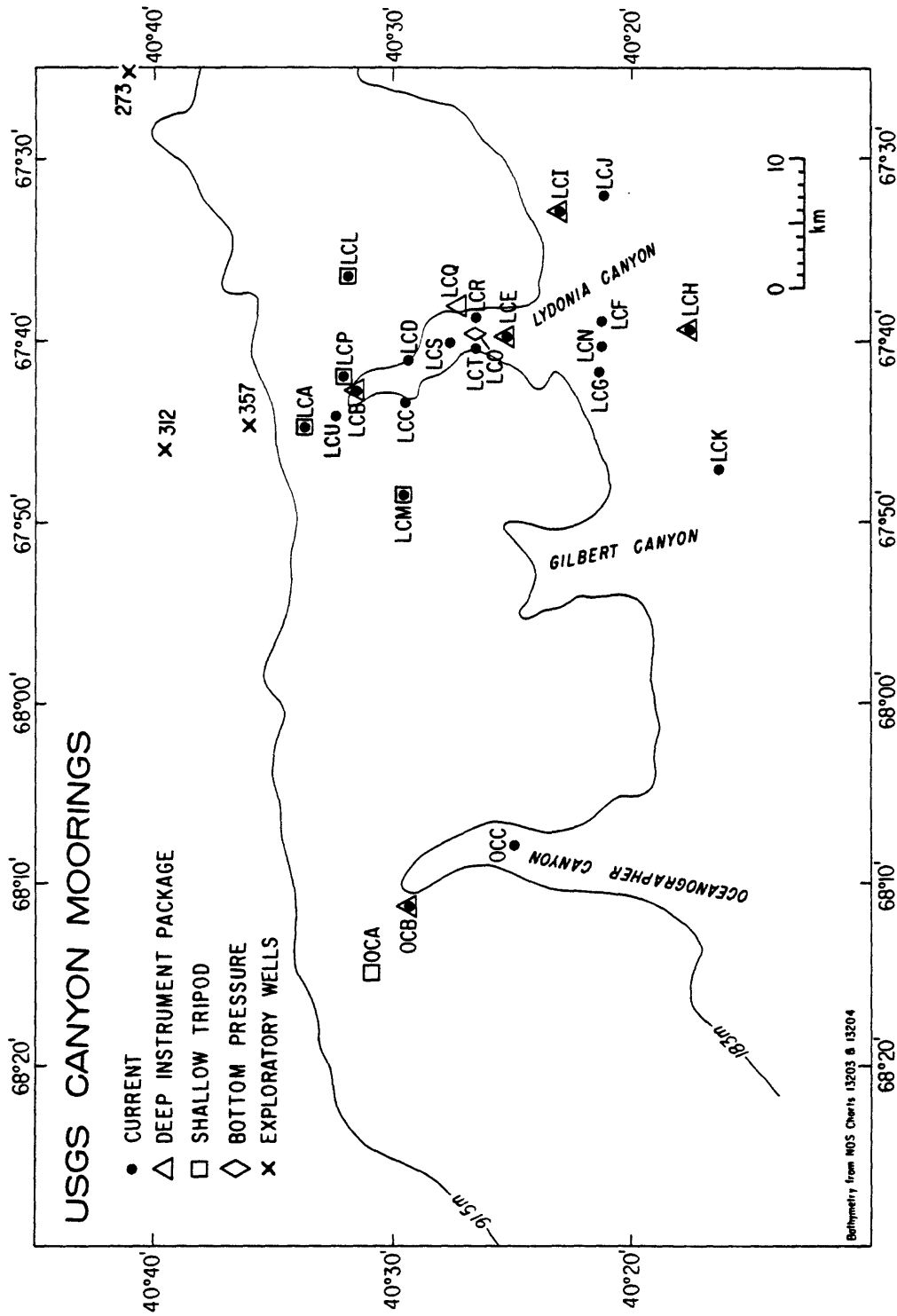


Figure 2a. Location of all moorings deployed as part of the Lydonia Canyon Experiment. The closest exploratory wells were drilled near Lydonia Canyon at Block 312 by Mobil between December 1981 and June 1982, at Block 357 by Shell between May and September 1982, and at Block 273 by Mobil between June and September 1982 (Danenberger, 1983).

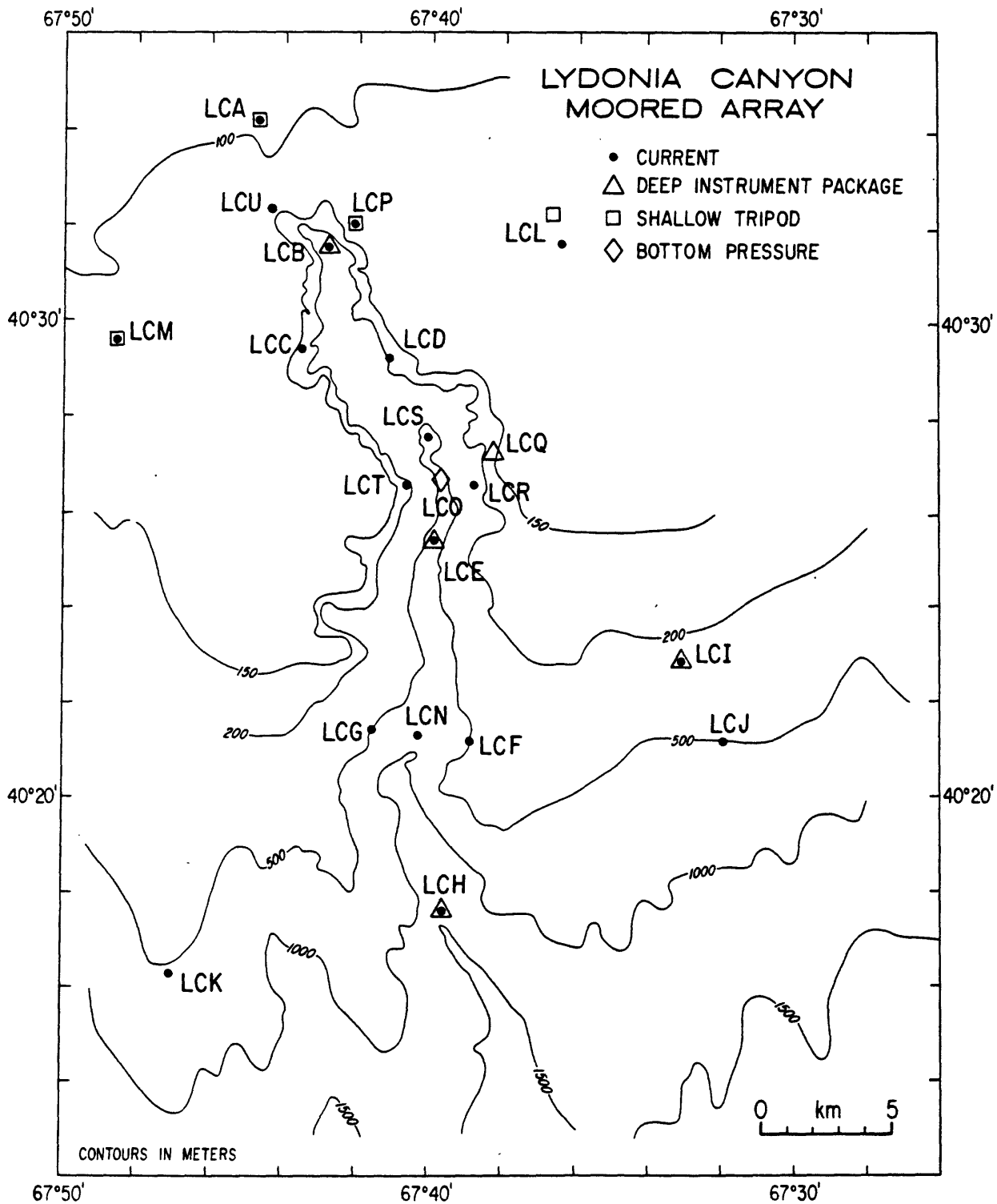


Figure 2b. Location of moorings deployed in Lydonia Canyon and on the adjacent shelf and slope. Not all stations were occupied simultaneously (see text).

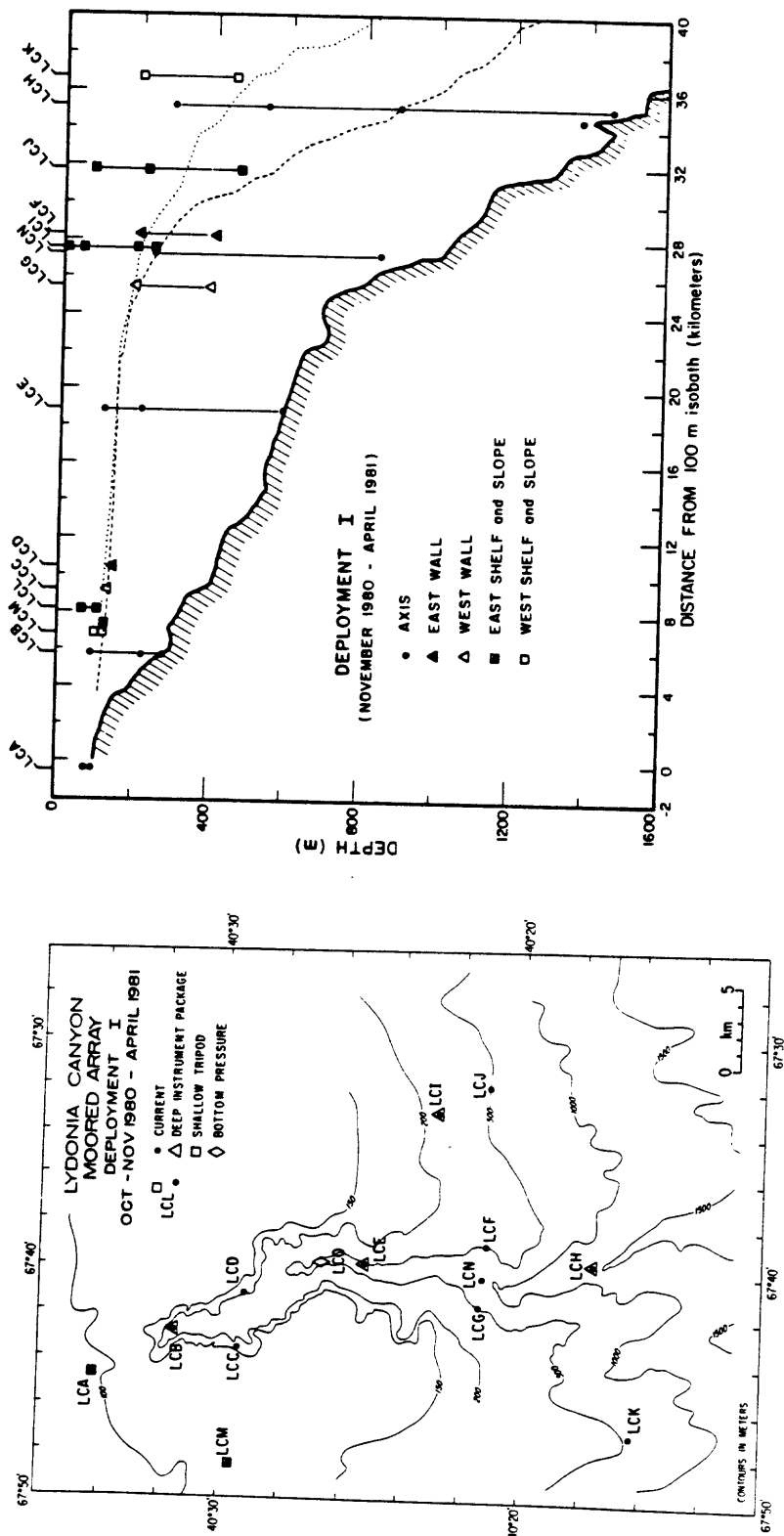


Figure 3. Base map and cross-section of Lydonia Canyon showing location of moorings and instruments in Deployment I of the moored array. Dotted (dashed) line indicates the slope to the west (east) of the canyon.

Hydrographic observations were made on all mooring deployment and recovery cruises, and on one cruise midway through Deployment I (table 1). The cruise track for OCEANUS 91 is typical for these hydrographic cruises (fig. 4); sections were made across the shelf both to the east and west of Lydonia, along the canyon axis, and across the axis, near both the mouth and head of the canyon. At each station, a Neil Brown Instrument Systems profiler was used to measure temperature, pressure, conductivity, light transmission (a measure of the amount of suspended material in the water), and oxygen. These hydrographic sections show the location of the shelf-water/slope-water front, the influence of Gulf Stream warm core rings, and the changes in the hydrographic structure between shelf and canyon.

EG&G Vector Averaging Current Meters (VACMs) deployed on taut subsurface moorings were used in the canyon experiment (fig. 5). Some of the VACMs were modified to also measure pressure, light transmission, or light transmission and conductivity (to determine salinity). Two specialized instrument packages were used to document near-bottom currents and sediment movement. A bottom tripod system that measured near-bottom current, temperature, pressure, and light transmission, and photographed the sea-floor was deployed at stations around the head of Lydonia Canyon (Butman and Folger, 1979; fig. 6). A second instrument package, which measured the same variables except pressure, was used in the canyon axis where the bottom tripod system was unsuitable because of the rough topography (fig. 7). Sediment traps of several sizes and shapes were deployed on the subsurface moorings to estimate particle flux and the physical and chemical composition of the suspended material.

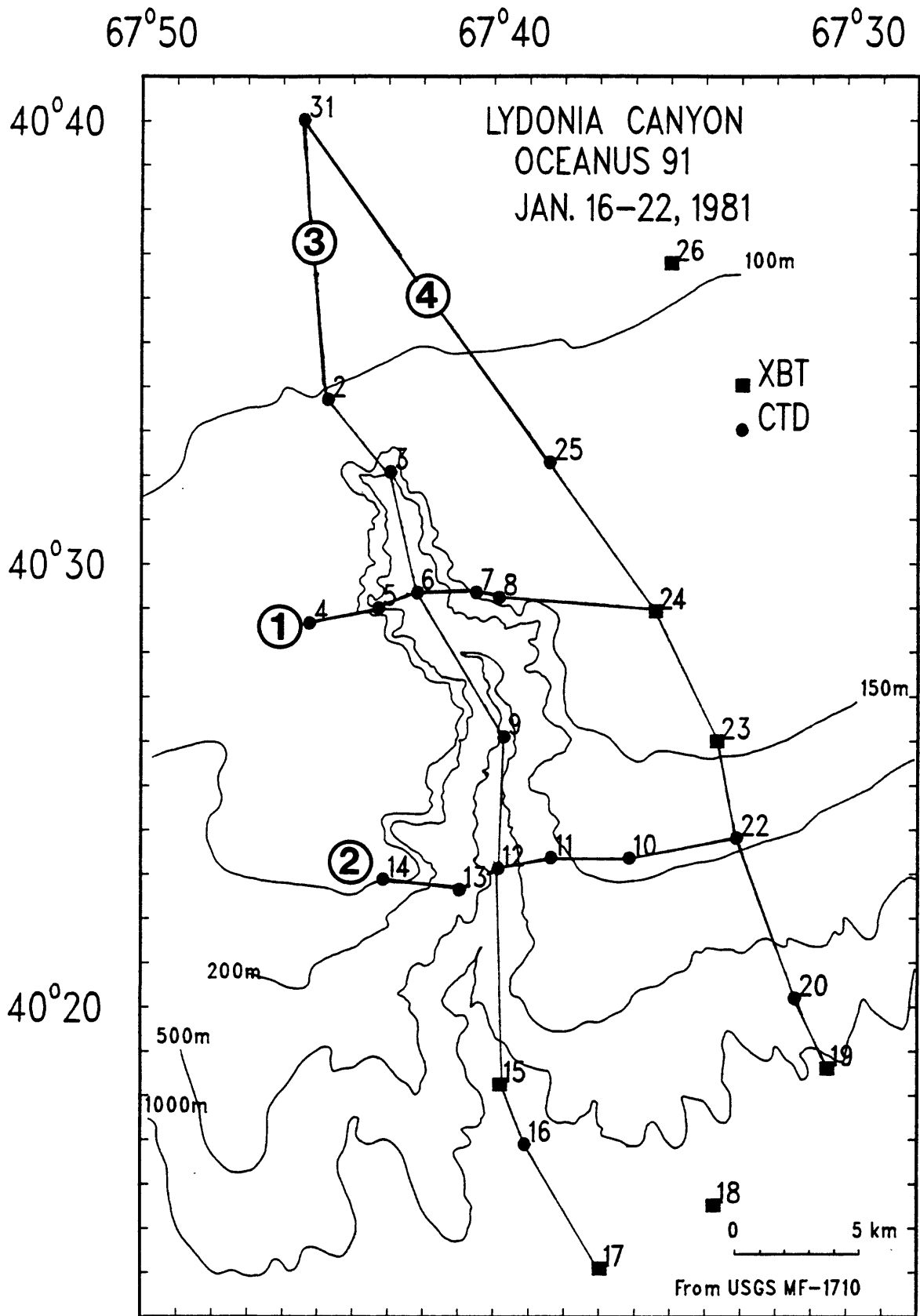


Figure 4. Cruise track for OCEANUS 91, typical of the hydrographic cruises made as part of the Lydonia Canyon Experiment.

MOORING 204 (TRIPOD)
 207 (SUBSURFACE)
 STATION LCA, SHELF
 LATITUDE : 40° 34.21' N
 LONGITUDE : 67° 44.55' W
 DEPTH : 100M

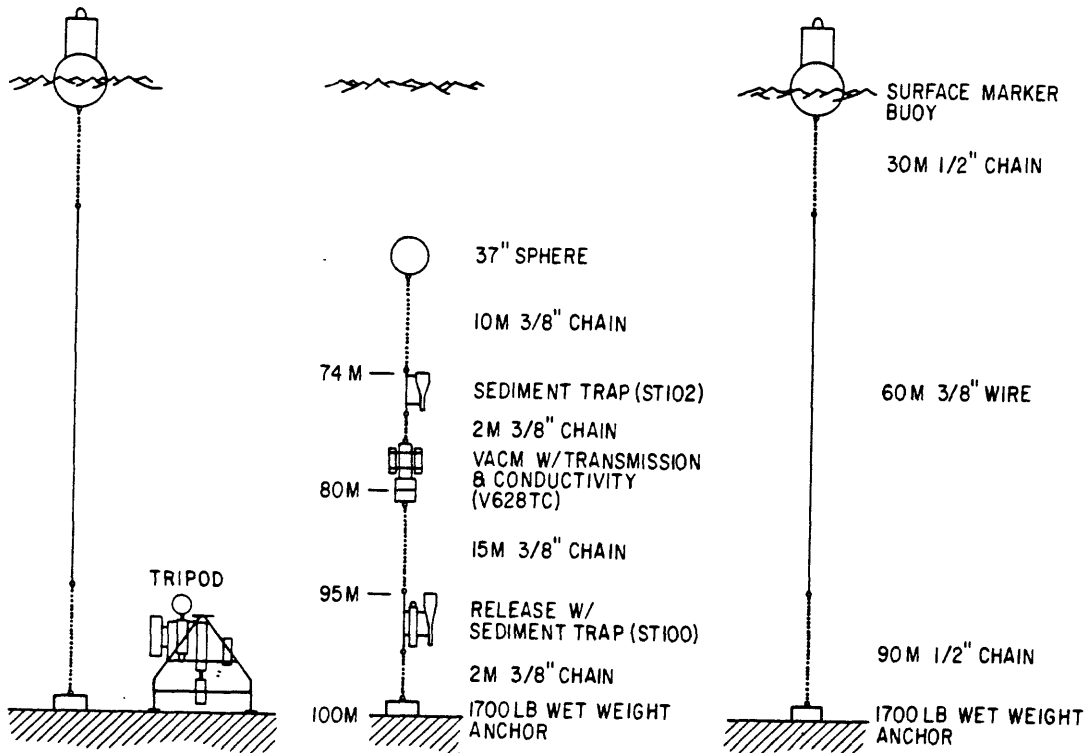


Figure 5a. Schematic of mooring 204 and 207 at LCA, typical of moorings deployed on the shelf as part of the Lydonia Canyon Experiment. The surface buoys mark the location to help fisherman avoid the site.

MOORING 211
 STATION LCE, CANYON AXIS
 LATITUDE : 40° 25.38' N
 LONGITUDE : 67° 39.88' W
 DEPTH : 600 M

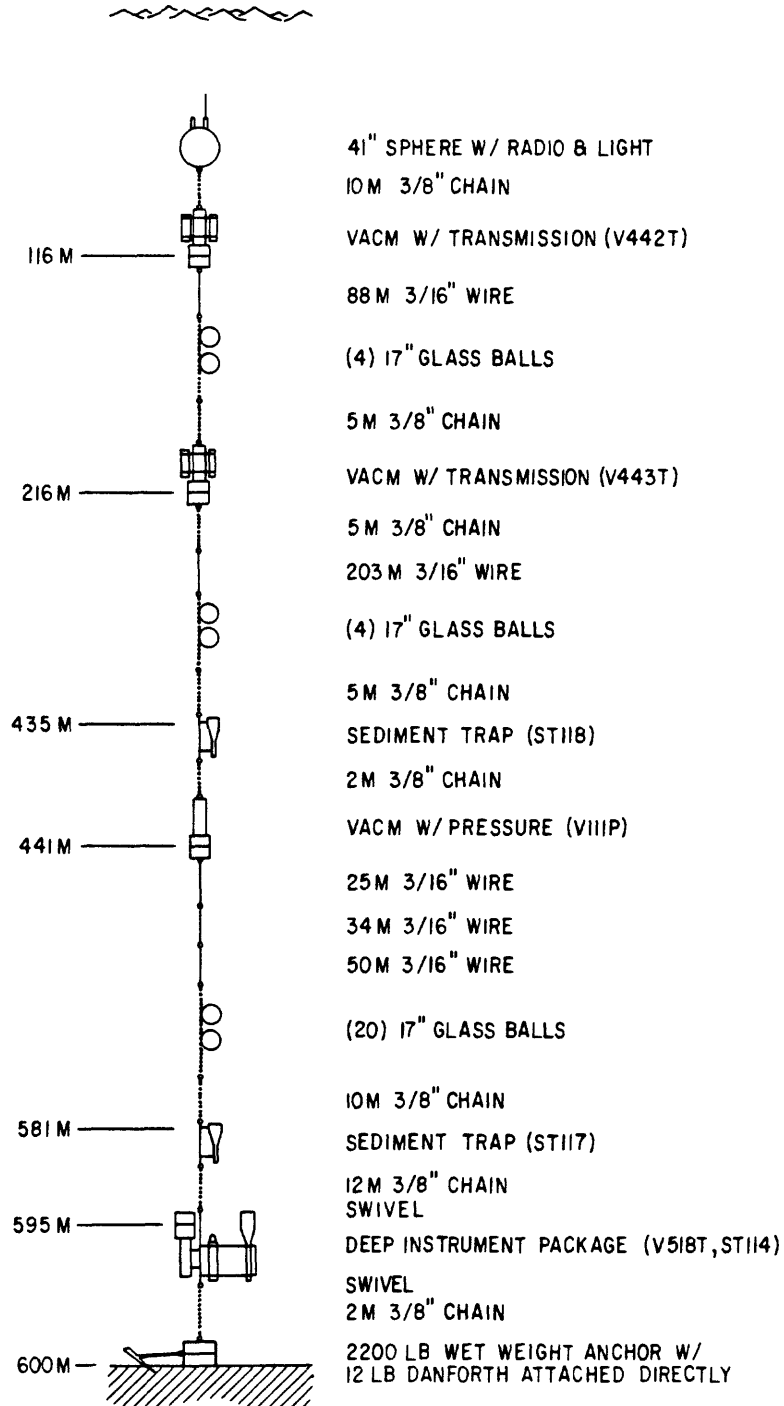
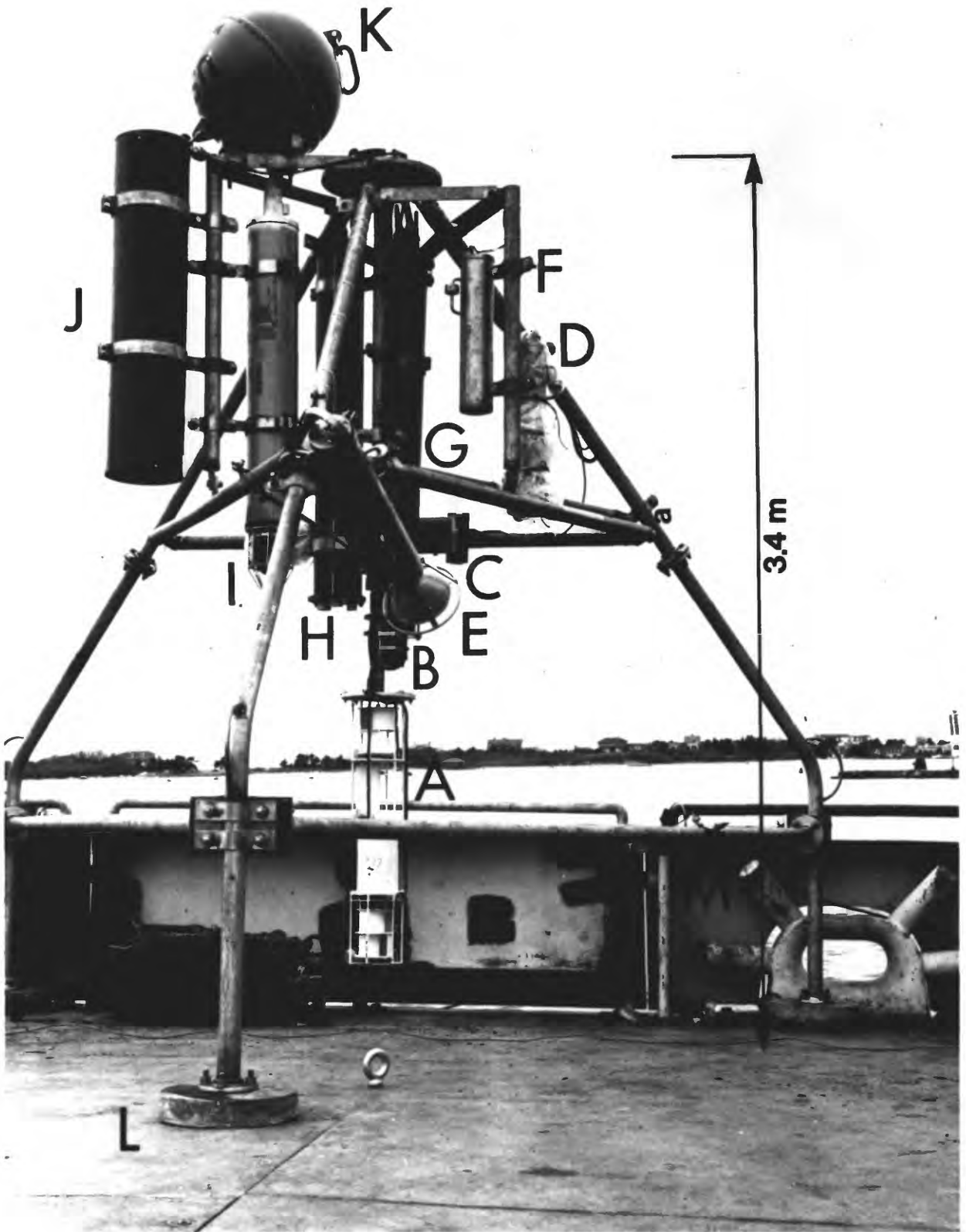
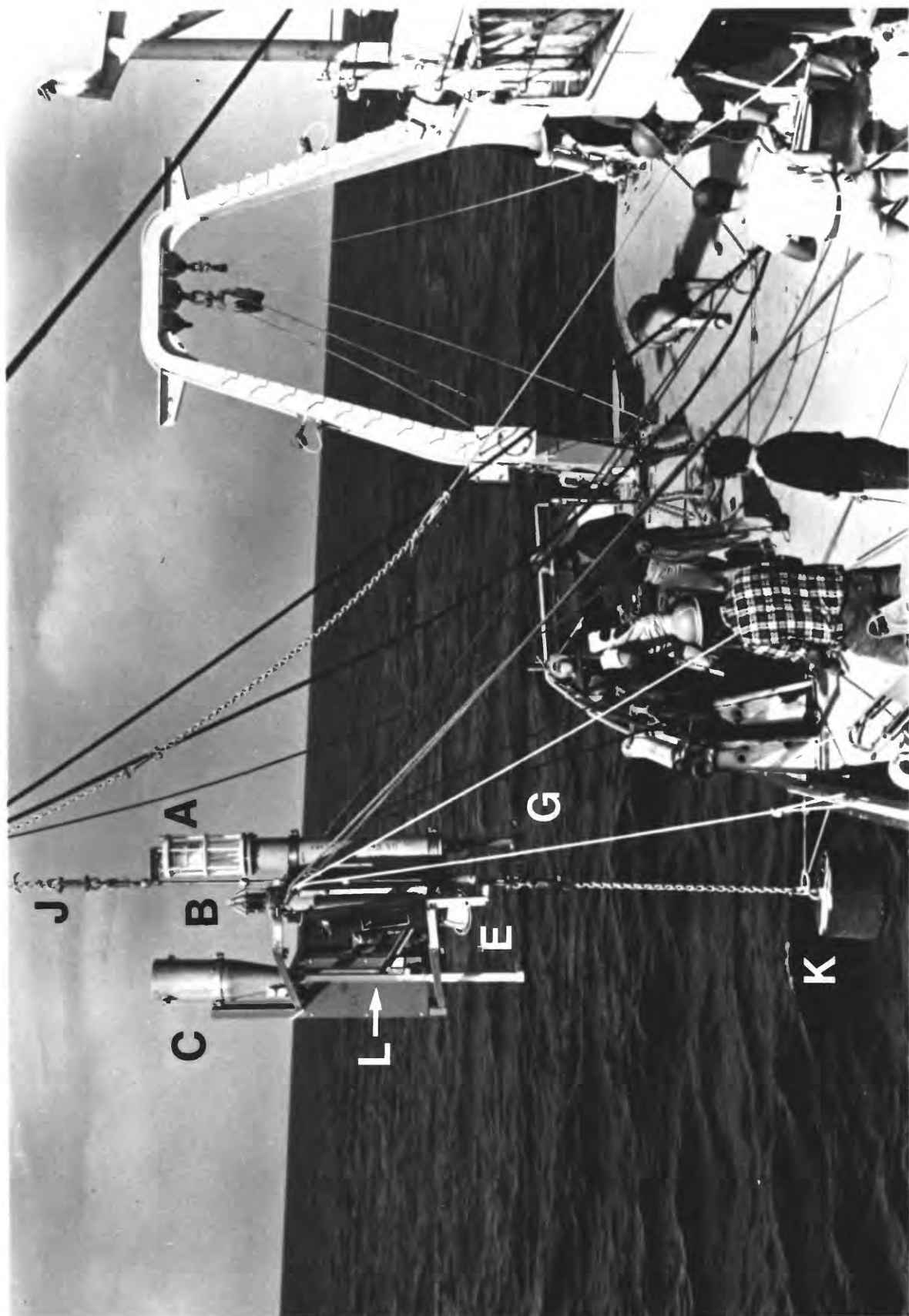


Figure 5b. Schematic of mooring at LCE, typical of moorings deployed in Lydonia Canyon and on the continental slope as part of the Lydonia Canyon Experiment.





Slope Experiment

The Slope Experiment included long-term measurements by an array of current meters and sediment traps and synoptic hydrographic observations. Three deployments of instruments were made between November 1982 and November 1984 (table 1; fig. 8). The instruments were deployed in two cross-slope transects, one near 69°30' W and one near 70° W. Additional moorings along the slope at 500 m were used to assess along-slope coherence and variability. Instruments were maintained at 100 meters above bottom (mab) at station SE and SA throughout most of the experiment to assess long-term variability. During deployment 3, moorings were deployed on a local topographic high (station SG) and in an adjacent topographic low (station SH) at about 1200-m water depth to compare these slope environments. Measurements of sediment texture and infauna were also made at these locations as part of the Study of Biological Processes on the North Atlantic Slope and Rise (Maciolek and others, 1986). Hydrographic observations were made on all mooring deployment and recovery cruises. The cruise track for OCEANUS 140, where eight sections were made across the outer shelf to the upper slope (fig. 9), is typical of the hydrographic cruises.

RESULTS

Canyon Geometry and Sediment Texture

Lydonia Canyon, as defined by the 200 m isobath, cuts northward into the northwestern Atlantic Continental margin approximately 20 km from the shelf edge (figs. 1, 10). The canyon is only a few kilometers (km) wide near the head and about 5 km wide near the mouth at the edge of the shelf. The canyon axis is sinuous, and there are numerous side gullies and spurs along the walls. Deep Submersible Research Vessel (DSRV) ALVIN dives show that the

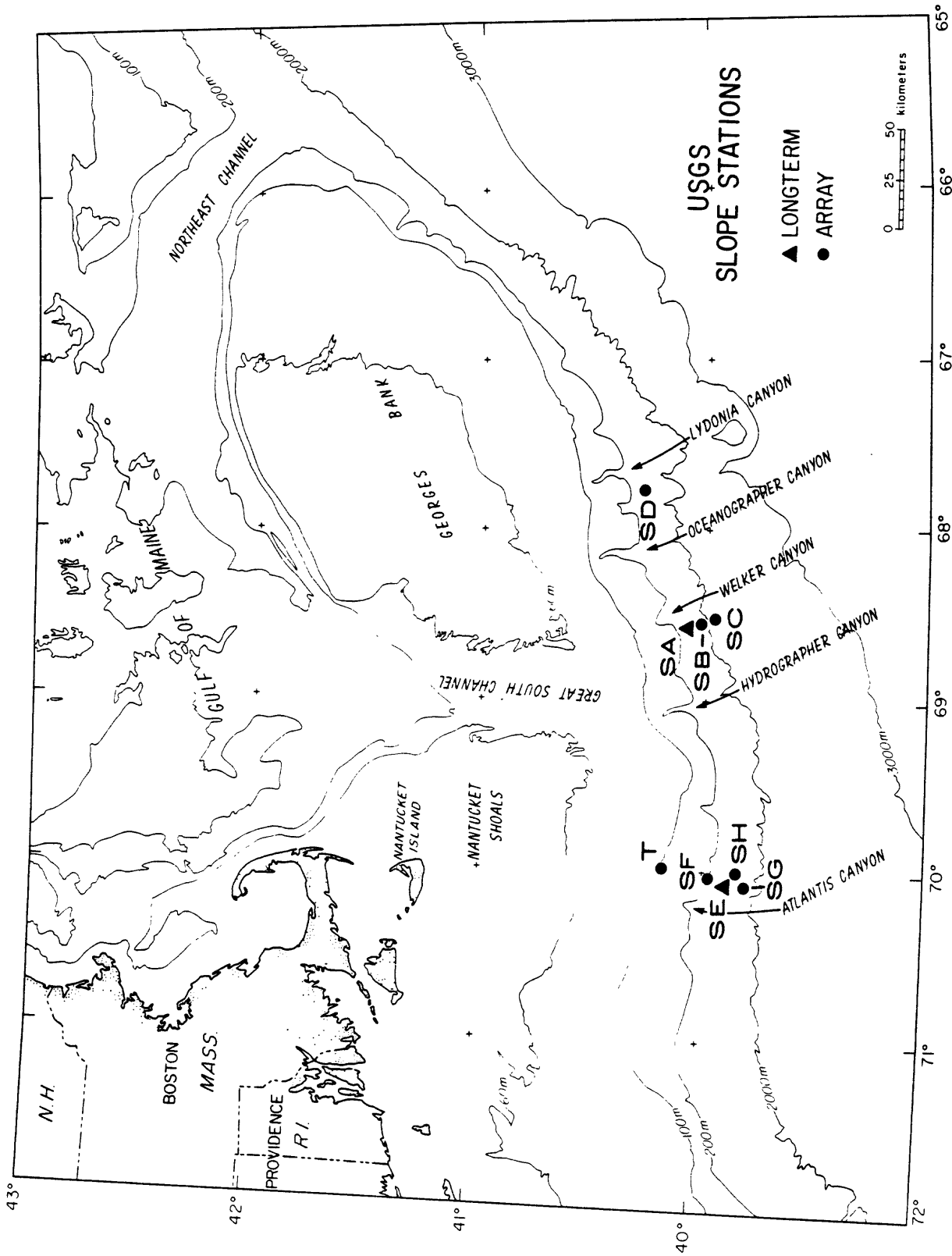


Figure 8. Locations of moorings deployed as part of the Slope Array Experiment. Not all stations were occupied simultaneously (see text and table 1).

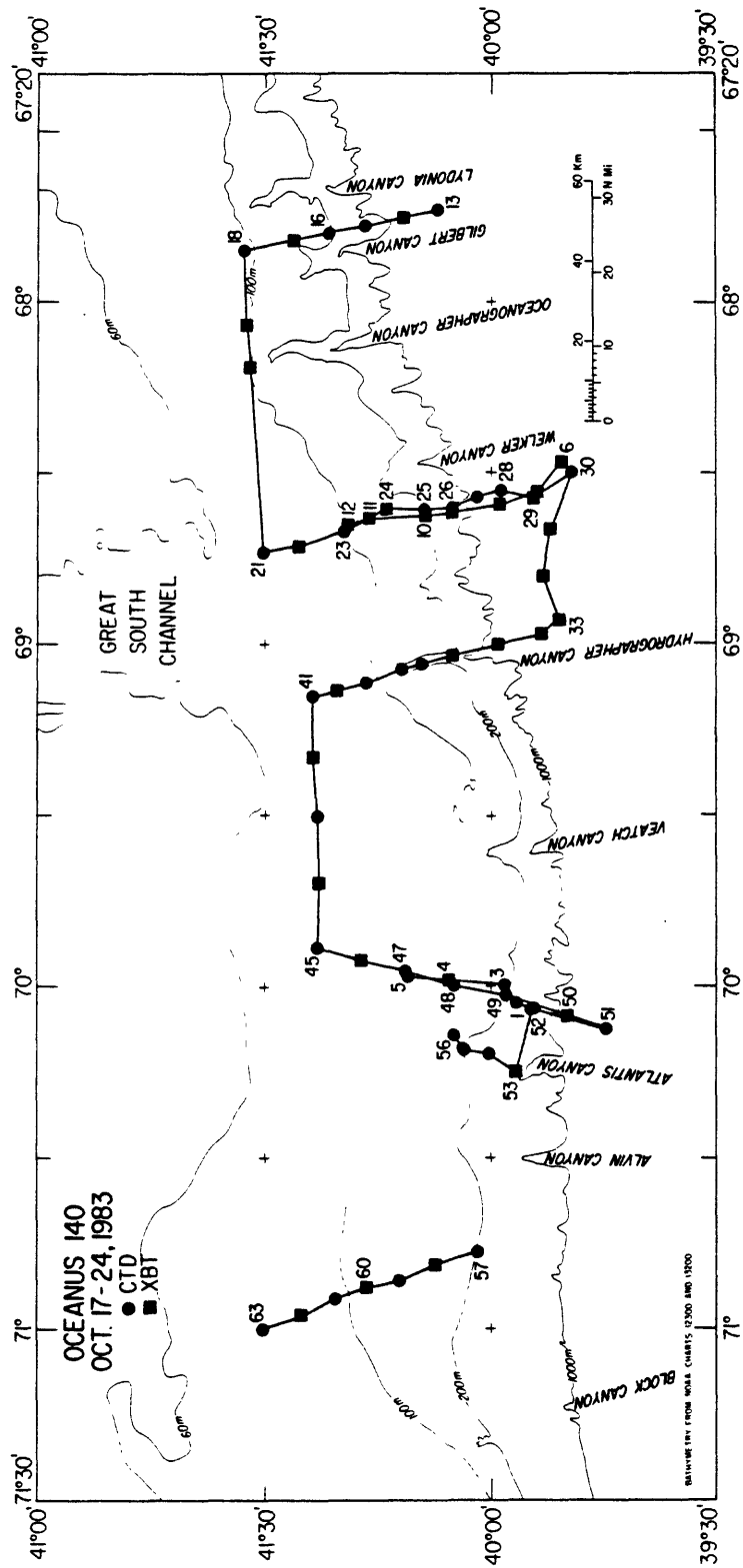


Figure 9. Cruise track of OCEANUS 140, typical of hydrographic cruises made as part of the Slope Experiment.

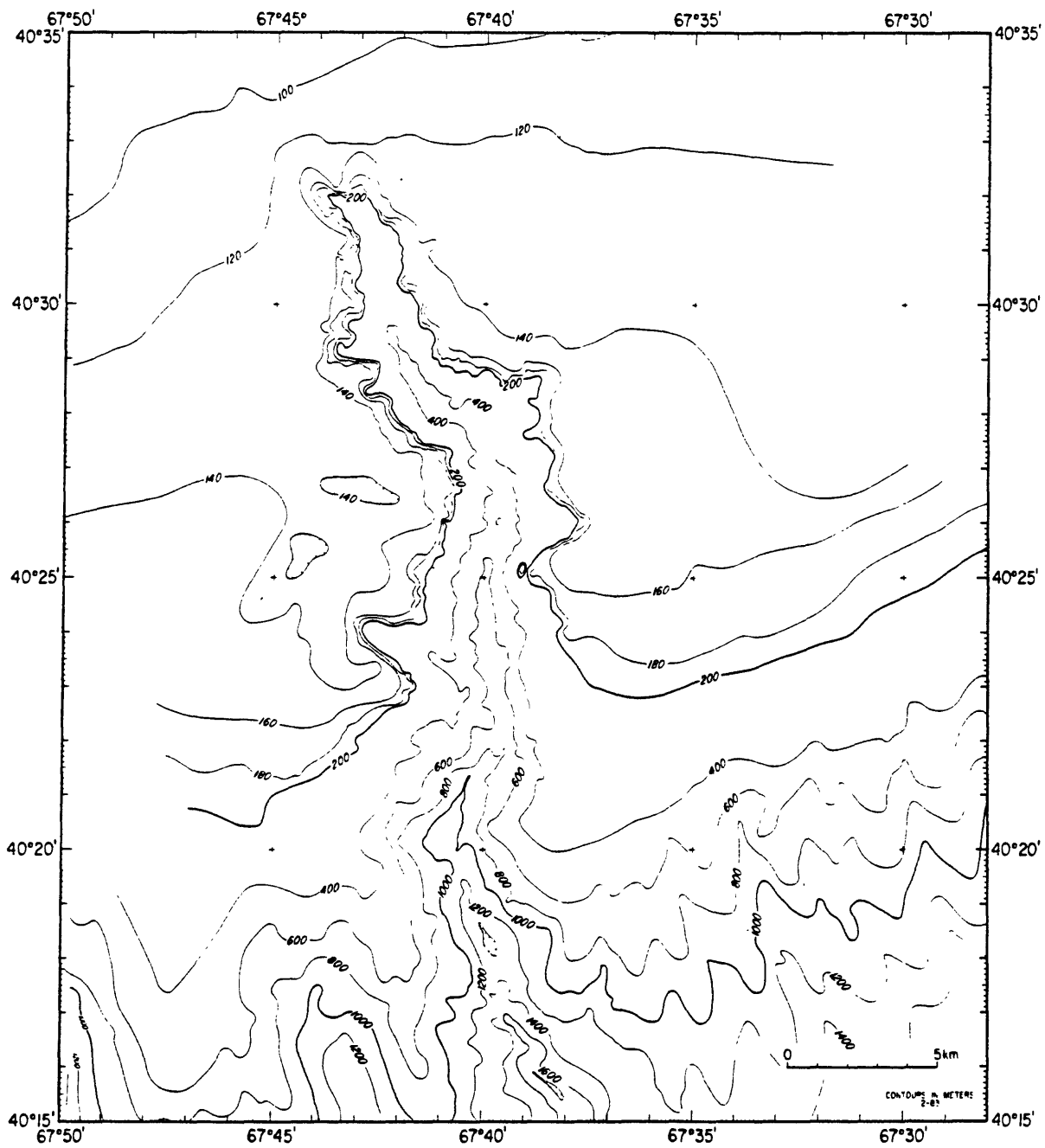


Figure 10. Bathymetric map of Lydonia Canyon (simplified from Butman and Moody, 1984).

canyon walls are almost vertical in some parts of the axis at axis depths below about 400 m. The average slope of the walls ranges from 10-20° while the slope along the axis floor is 1-5°.

The surficial sediment on the southern flank of Georges Bank becomes gradually finer to the west and toward deeper water, primarily reflecting the strength of the tidal currents (Butman, in press). Superimposed on this regional pattern are smaller scale changes apparently associated with the canyons. Finer grained sediments, primarily very fine sand and silt, occur in lobes about 10 km wide both to the east and west of Lydonia Canyon (fig. 11). Along the axis of the canyon, there are significant changes in the texture of the surficial sediments. Increased concentrations of silt plus clay occur near the head around LCB and coarser sediments near LCS and LCE (fig. 12). At depths greater than 600 m, the sediments are progressively finer with depth; there is almost no sand at 1600 m.

Based on high-resolution seismic-reflection profiles, Twichell (1983) inferred that the finer-grained sediments near the canyon head are of Holocene age, that they are as much as 25 m thick and, in some places, are draped over the existing topography. Cores obtained near LCU show accumulation rates of about 60 cm/1000 yrs. Thus the geological and geochemical information--sediment texture, geometry, and accumulation rates--which reflect the net transport of sediment over thousands of years, show that sediments are accumulating in the head of Lydonia Canyon, at least at depths shallower than about 500 m. The fine sediments deep in the canyon also imply accumulation there.

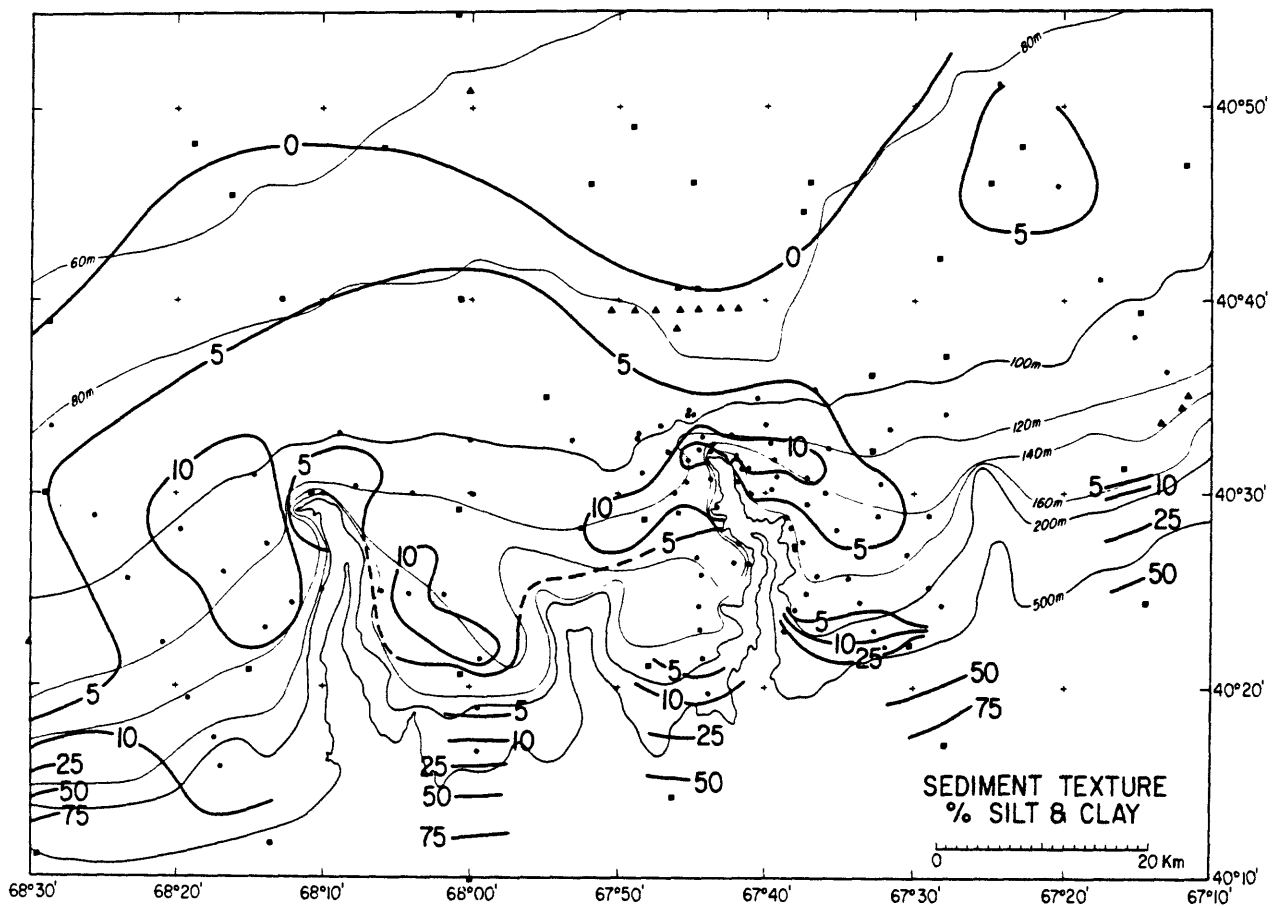


Figure 11. Percent silt plus clay in the surficial sediments on the southern flank of Georges Bank near Lydonia and Oceanographer Canyons. Triangles are samples reported by Bothner and others (1985) and squares from Hathaway (1971). Circles are samples collected from this study. Surface texture in the canyons at depths greater than 200 m is not shown in this figure.

AXIS OF LYDONIA CANYON SURFACE SEDIMENT TEXTURE

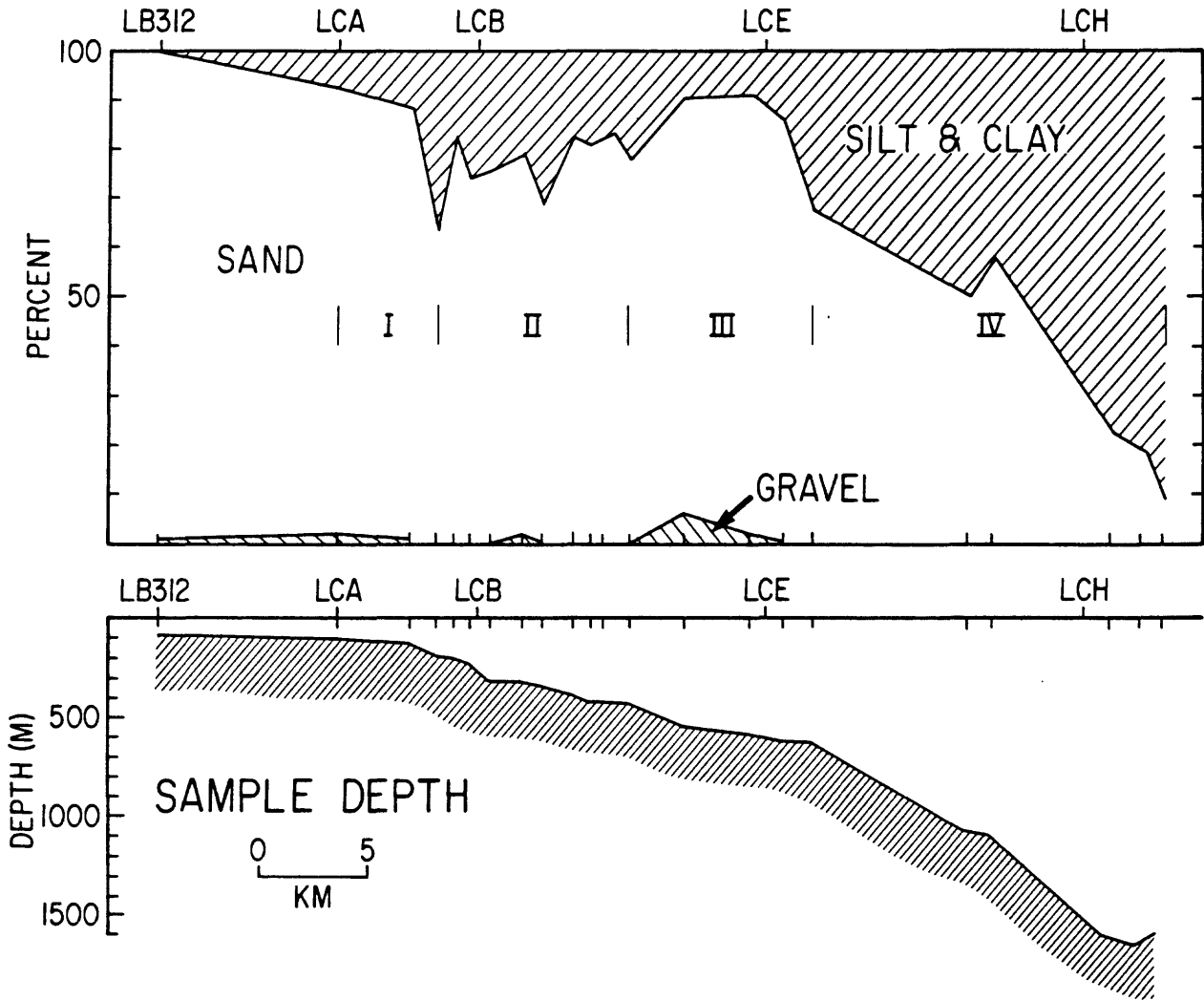


Figure 12. Surficial sediment texture along the axis of Lydonia Canyon. Samples were obtained from the submersible ALVIN.

Currents

The current observations made in Lydonia Canyon and on the shelf and slope show a rich diversity in the strength, orientation, and frequency of current fluctuations. Within the canyon, the currents are channelled by the topography. Currents oscillate up and down-canyon, primarily at the semidiurnal tidal period. These current fluctuations are not always in phase with the well-defined tidal currents on the shelf, and the amplitude of the fluctuations changes with time. The fluctuations sometimes occur in short bursts or packets of a few days duration. The current fluctuations are also not symmetric in time (i.e., the strength and duration of the up-canyon flow is not the same as the down-canyon flow) especially toward the canyon head. This asymmetry in flow, which has important implications for the transport of sediment, probably results from the complicated topography, bottom slope, and stratification of the water in the canyon. Current fluctuations are intensified toward the bottom in the canyon.

Above the canyon rim and on the shelf landward of the shelf break, the currents are dominated by the semidiurnal tidal currents which flow across isobaths, and by low-frequency currents, some caused by winds, which are oriented parallel to the isobaths. There is also a well-defined weak residual flow toward the southwest at 1-5 cm/s. The canyon apparently has little effect on the mean, tidal, or low-frequency currents above the rim.

On the slope, the currents at water depths between about 150 m and 500 m are strongly influenced by the currents associated with Gulf Stream warm core rings (fig. 13a). These rings are about 100 km in diameter and are formed from northward meanders of the Gulf Stream. The rings drift slowly westward in the slope water until they are reabsorbed by the Gulf Stream near Cape Hatteras or by interaction with meanders of the stream (Lai and Richardson,

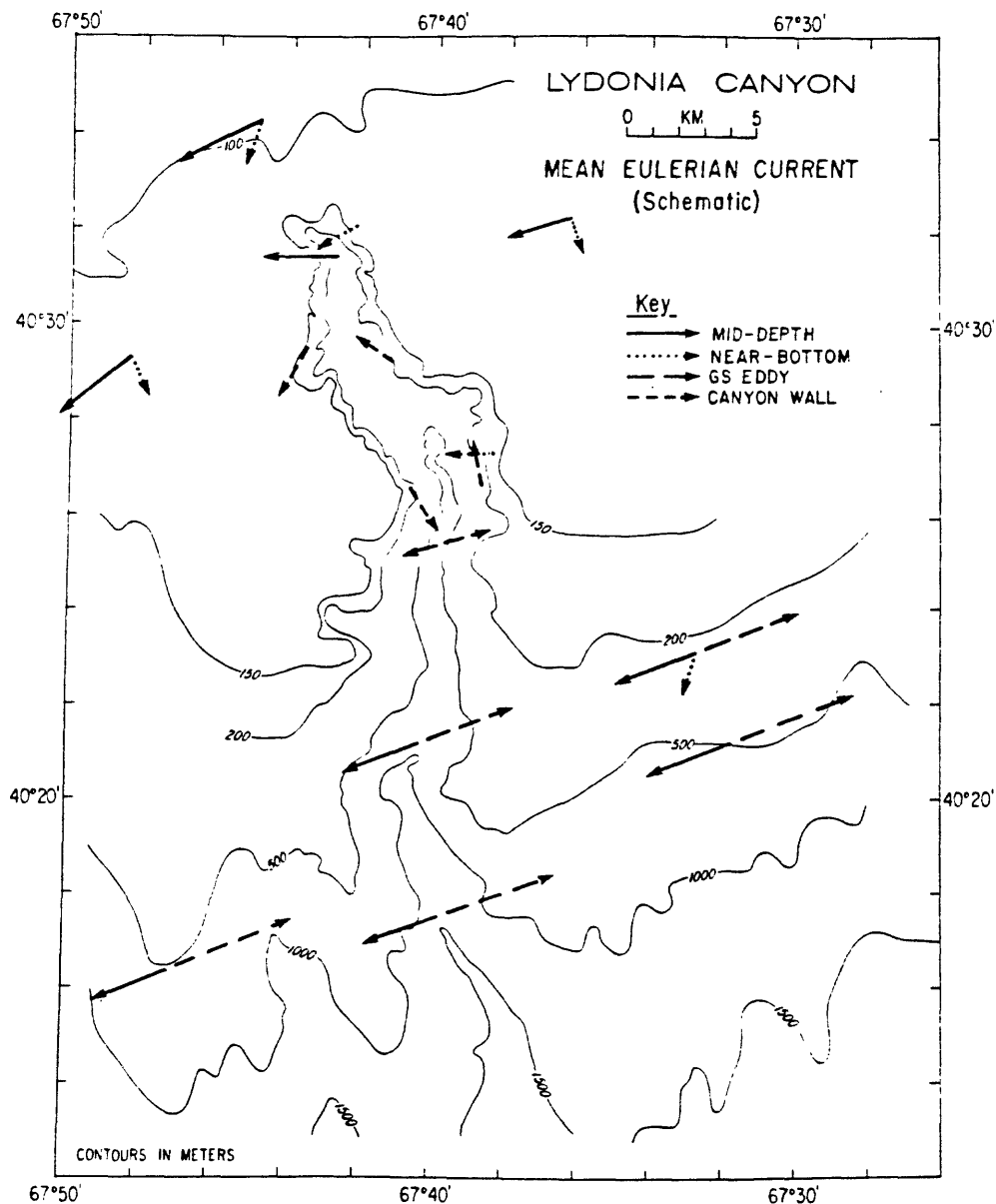


Figure 13a. Preliminary schematic of the Eulerian mean flow on the shelf and slope adjacent to Lydonia Canyon and along the walls of the canyon. Solid lines indicate the mid-depth flow and dotted lines the near-bottom flow. On the slope, the arrows indicate flow in the upper 100-200 m. The heavy dashed lines indicate the mean flow when Gulf Stream eddies are located to the south of the canyon and the solid lines indicate flow in the absence of eddies. The light dashed lines indicate flow along the canyon wall just below the level of the adjacent shelf (at about 150 m at the two locations in the head of the canyon, and at about 200 m at the two stations near the mouth of the canyon).

1977; Halliwell and Mooers, 1979; Richardson, 1983; Joyce, 1984; Beardsley and others, 1985; Butman, in press). The clockwise circulation around the rings, sometimes at speeds approaching those in the stream, causes strong eastward flow along the outer edge of the shelf when the rings drift close to the shelfbreak. During the Lydonia Canyon Experiment, warm core rings affected the flow along the outer shelf and upper slope about 30 percent of the time. During the strongest ring events, eastward currents exceeded 80 cm/s and influenced the flow to about 500 m along the upper slope. Eastward flows extended shelfward to about the 150-m isobath at depths above the canyon rim (LCE) but not to the 110-m isobath (LCB). Rings may affect the flow within the canyon by generating packets of high-frequency current fluctuations. Near the bottom over the slope at LCI, SA, SE, and SF, there was a persistent downslope Eulerian mean flow.

Along the canyon axis, the net flow near the bottom was down-canyon at LCB and up-canyon at LCS (fig. 13b). Net flow was up-canyon at 50 mab at LCB and was down-canyon 100 mab at LCE. These observations suggest a bottom-intensified residual circulation that traps material in the canyon head. Net near-bottom flow at LCE and LCH was weak and not significant. Along the walls of the canyon at about 200 m, the observations suggest inflow along the eastern side (at LCF, LCR, and LCD) and outflow on the western side (at LCC, LCT, and LCG).

The convergence in the mean near-bottom flow toward the canyon head is one of the most important observations of the canyon experiment. However, current measurements made at fixed locations, called Eulerian measurements, do not always indicate the net transport of water or particles (called the Lagrangian current) if there are large vertical or horizontal changes in the current field. For example, water particles could travel past the current

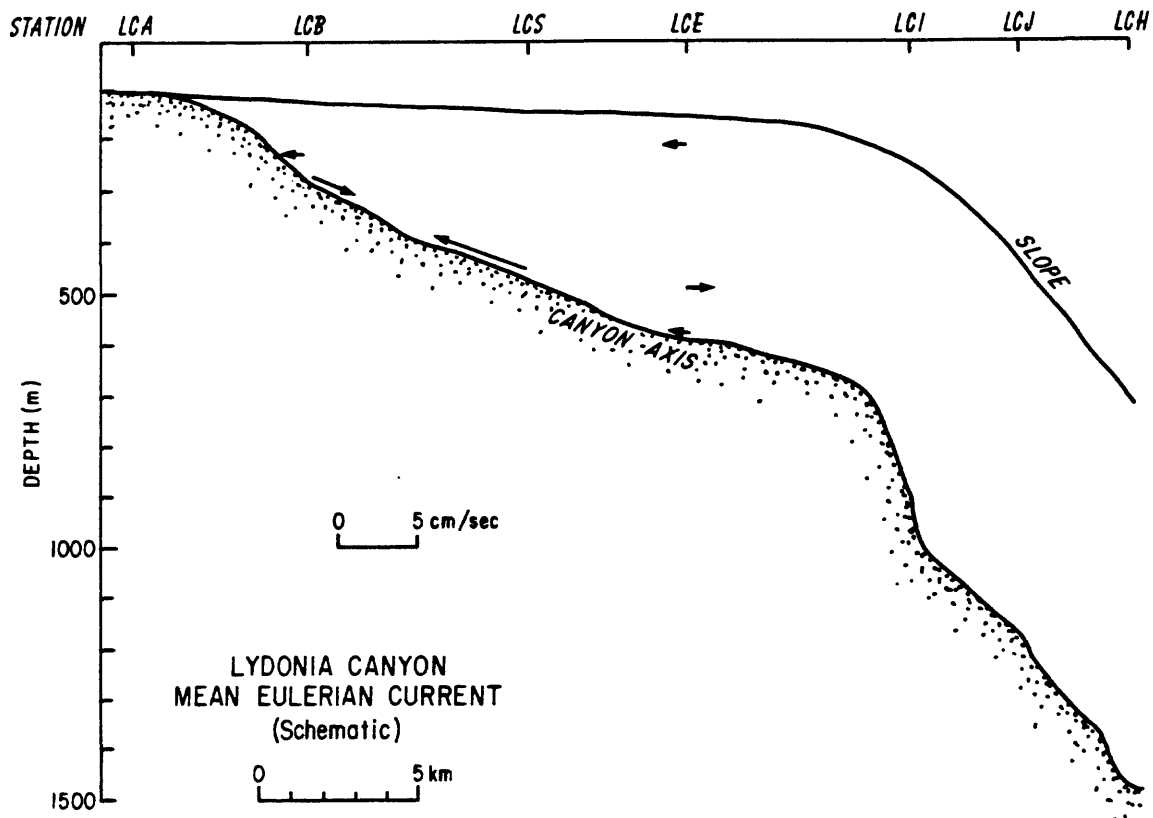


Figure 13b. Preliminary schematic of Lydonia Canyon showing upcanyon-downcanyon component of the mean Eulerian current at LCB, LCS and LCE along the canyon axis. Note that the mean Eulerian current may not indicate actual Lagrangian water-particle trajectories. The convergence in the near-bottom flow between LCS and LCB may partially cause the deposit of fine-grained sediments which occur in the upper part of the canyon. If the Eulerian and Lagrangian mean flow are equivalent, the convergence also suggests outflow between about 300-400 m, or small closed recirculation cells along the bottom. Data on the adjacent shelf and slope suggests westward flow across the canyon above the level of the canyon rim.

meter and recirculate in relatively small vertical or horizontal cells. The increase in the residual flow toward the bottom along the axis, where the current fluctuations are also largest, suggests that the observed net Eulerian flow is not the trajectory of water particles. The Eulerian flow probably does reflect the direction of transport of sand (see below).

The near-bottom current speeds (fig. 14) qualitatively reflect the surficial sediment texture in Lydonia Canyon (fig. 12). Currents were weakest deep in the canyon at 1600 m at LCH, where there is no evidence for active sediment movement and the sediments are all silt and clay. Currents were stronger near the canyon head, and were strongest at about 600 m where the sediments were coarsest.

Distribution of suspended particles

The hydrographic sections along the axis (fig. 15), the moored transmissometer observations, and the sediment trap observations (fig. 16) all indicate increased sediment concentrations in the water near the bottom toward the head of the canyon. The profiles of beam attenuation show an increase in particle concentrations in a layer 50 to 100 m thick above the bottom, and the moored observations show that the concentrations of suspended sediments near the bottom change rapidly with time as fine particles are resuspended or advected past the instrument from elsewhere in the canyon (fig. 17, 18). The amount of material caught in the sediment traps increased logarithmically toward the bottom at LCB, suggesting frequent local resuspension. The head of Lydonia Canyon might be described as an "active sink", where fine particles not only accumulate, but are also frequently resuspended from the seafloor. This resuspension may allow fine particles to strip dissolved pollutants from the water column. Increased inventories of ^{210}Pb and $^{239,240}\text{Pu}$ in the

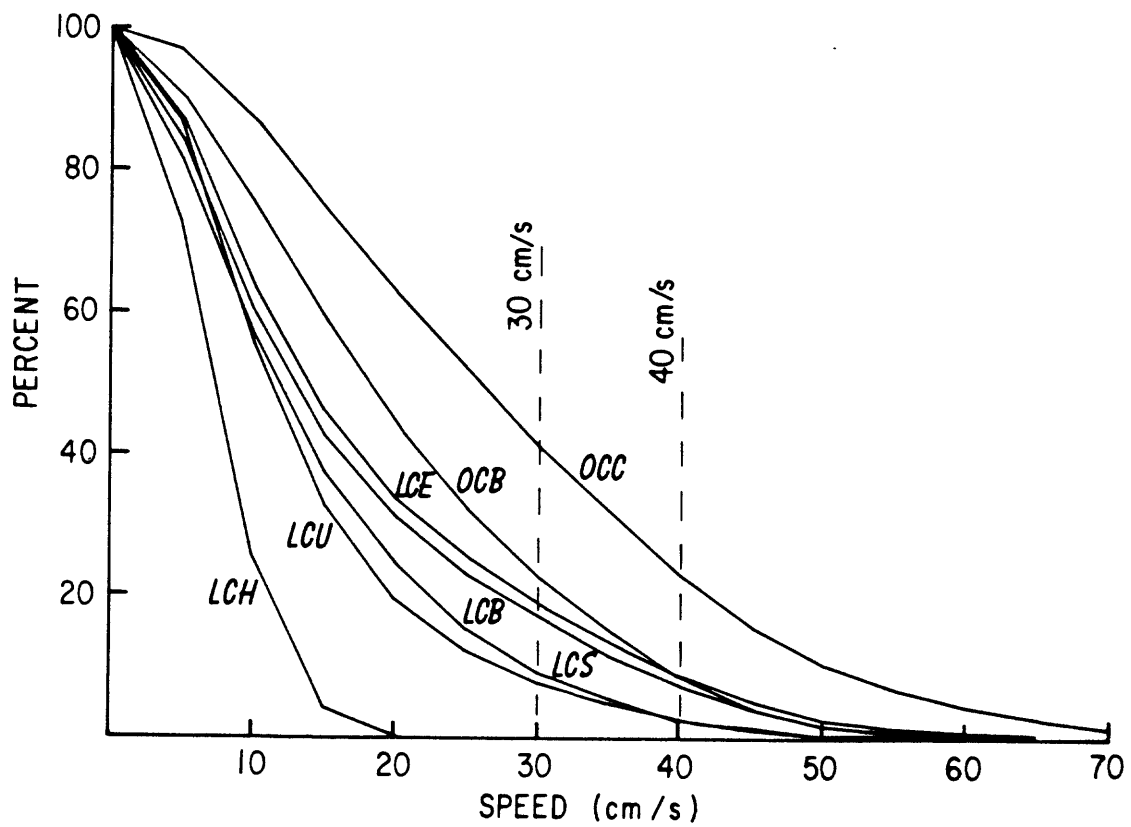


Figure 14. Histogram of near-bottom currents at stations along the axis of Lydonia and Oceanographer Canyons (fig. 2). The curves show the percent of time that the current exceeds the speed given along the X-axis.

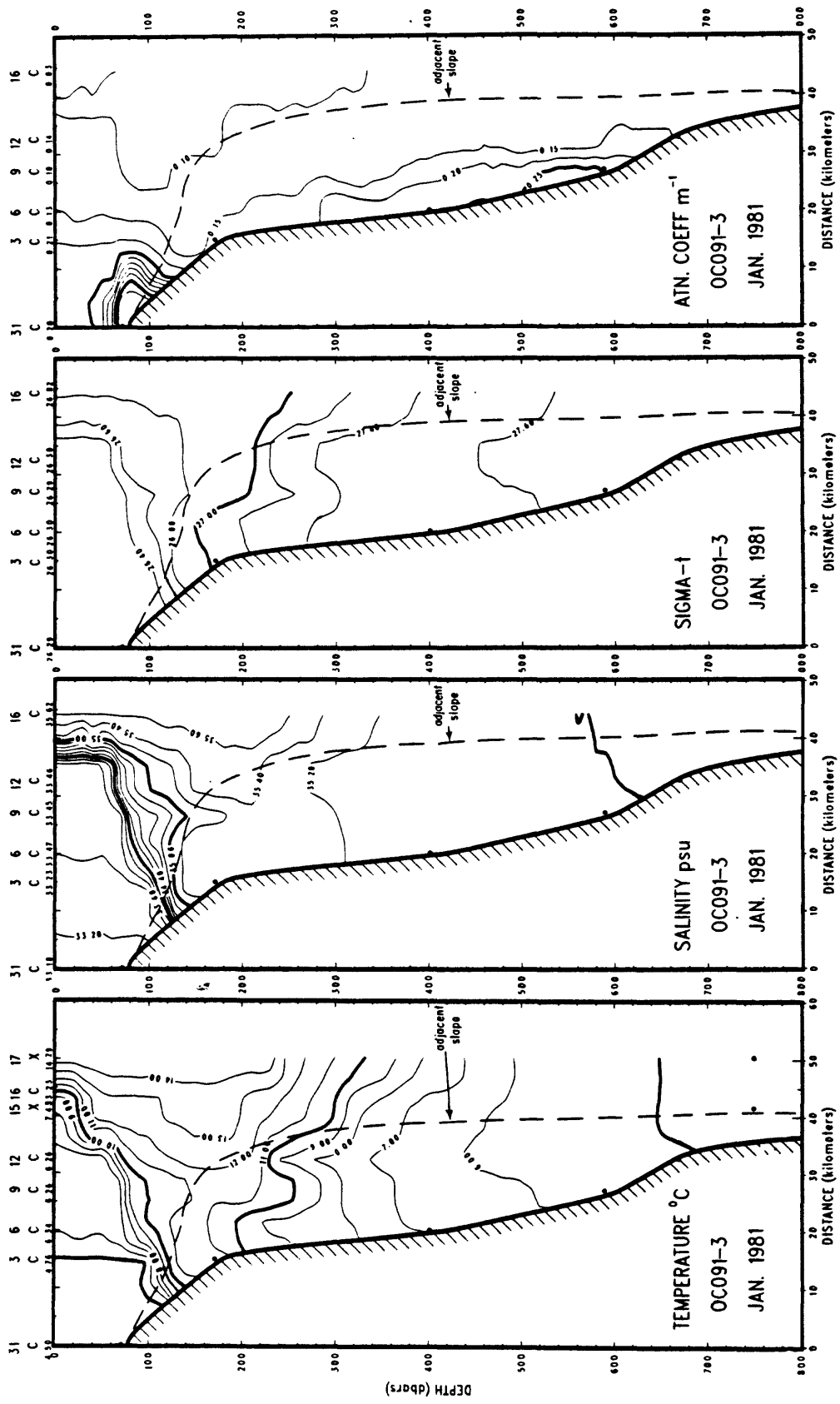


Figure 15. Hydrographic section along the axis of Lydonia Canyon made in January 1981 showing temperature, salinity, sigma-t (density) and beam attenuation coefficient (proportional to suspended sediment concentration).

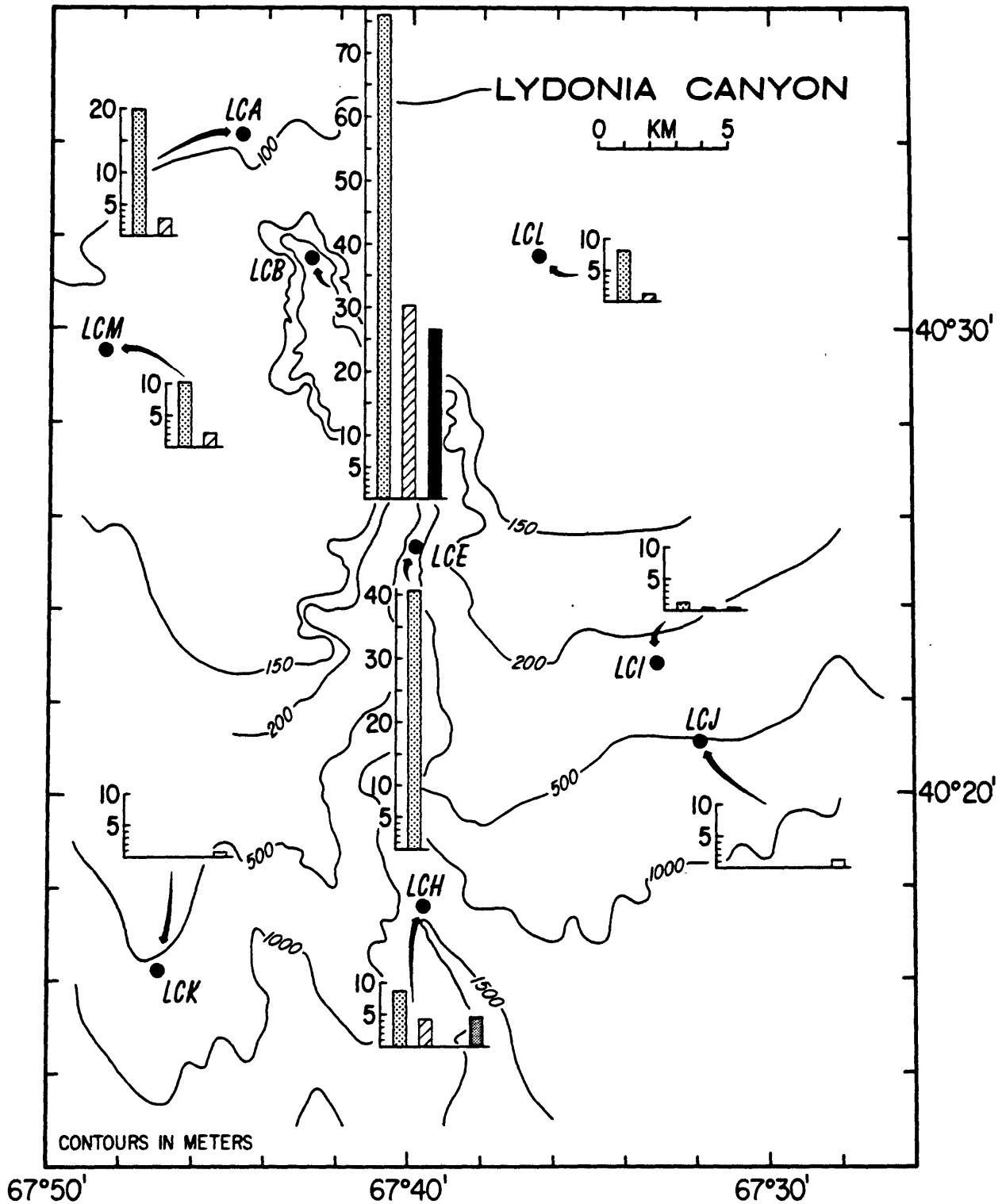


Figure 16. Histograms showing the flux of resuspended sediment ($\text{g/m}^2/\text{day}$) at different heights above the bottom; = 5 mab; = 20-26 mab; = 50 mab; = 100 mab; = 300 mab.

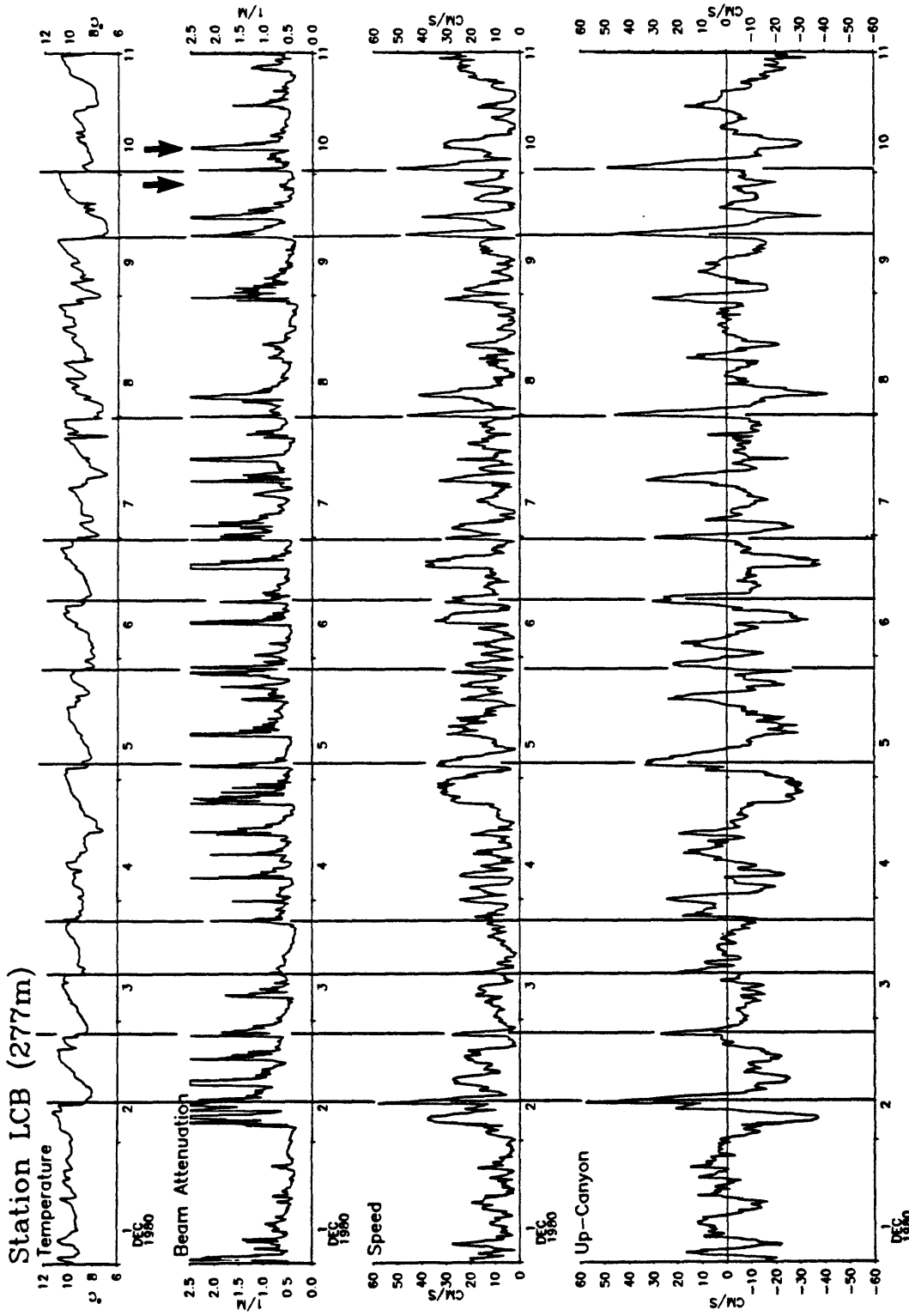


Figure 17. Time series of temperature, beam attenuation, bottom current speed, and up-canyon component of flow 5 meters above bottom at LCB between December 1 and December 10, 1980. The observations illustrate the rapid changes in suspended sediment concentrations and the asymmetric flow in the canyon. Arrows indicate times of photographs shown in figure 18.

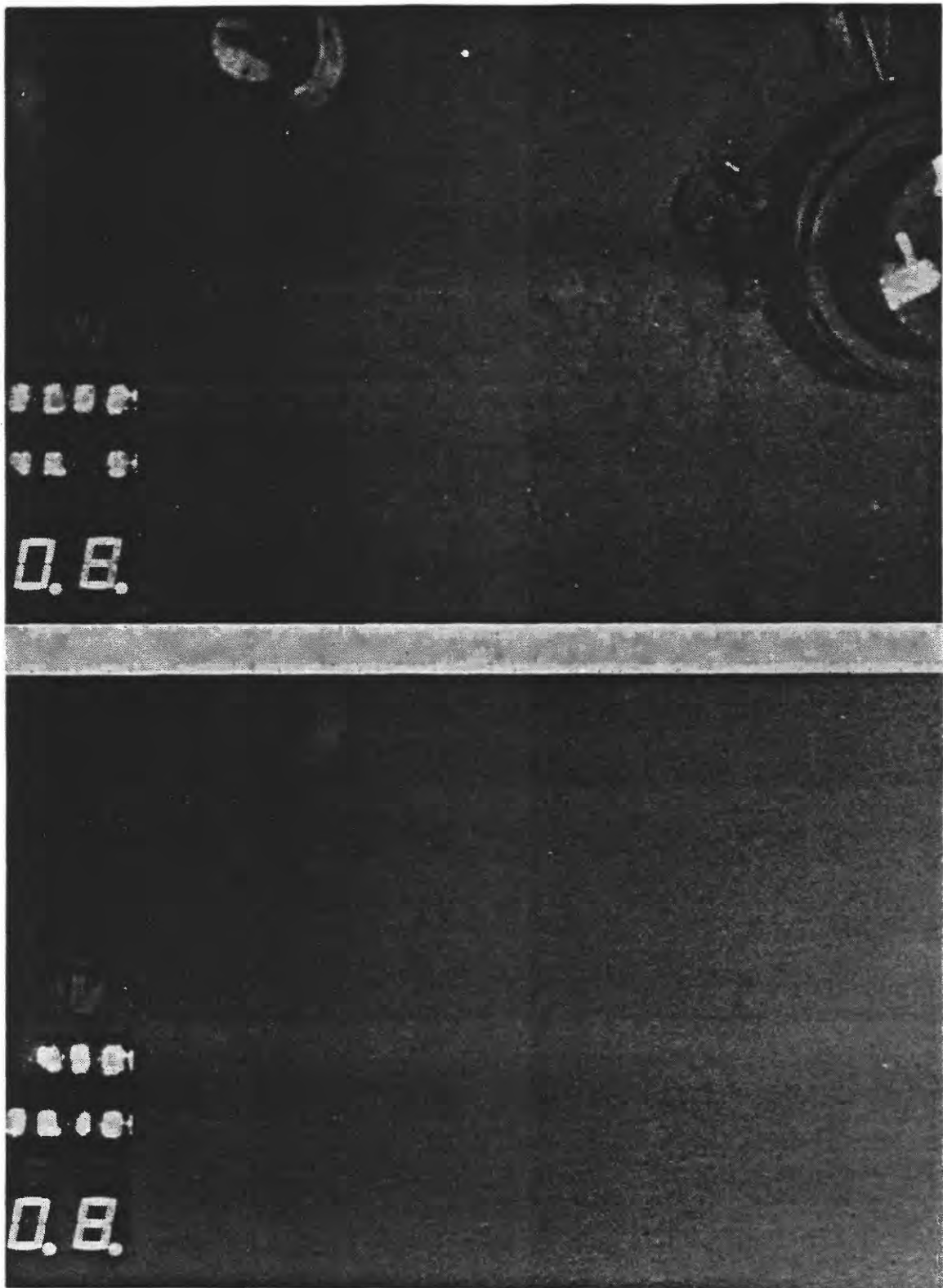


Figure 18. Bottom photographs at LCB obtained by means of Deep Instrument Package showing typical bottom microtopography. The anchor is about 81 cm (32") in diameter. The top photograph was obtained Dec. 9 at 2302 EST. Up-canyon is toward the top of the photograph. The bottom photograph was obtained Dec. 10 at 0458. Suspended sediment concentration is so large that bottom is obscured from view. See figure 17 for time series data obtained at same period. The photographs illustrate the large sudden changes in suspended sediment concentrations typical of the canyon axis.

surficial sediments in the axis are consistent with this hypothesis.

Sediment transport

The transport of sand-sized material along the axis of Lydonia Canyon and on the adjacent shelf and slope was calculated using the current observations and a one-dimensional model of sediment transport in the bottom boundary layer (based on Grant and Madsen, 1979; Grant and Glenn, 1983). The calculated transports show a net down-canyon transport of sand at the head of the canyon (at LCU and LCB) and up-canyon transport at LCS (550 m). The calculated transports qualitatively agree with the measured accumulation rates. Most of the along-axis transport is caused by the asymmetrical tidal and higher frequency current fluctuations. At 1600 m, there was no resuspension or transport of the existing sediments.

Storms resuspend sediment on the continental shelf. On the southern flank of Georges Bank, the resuspended sediment is carried primarily parallel to the shelf isobaths and may intersect the canyon rim. This is most likely when the flow over the shelf is to the southwest and the near-bottom flow is also slightly off-shelf (down-welling). This storm transport should be largest in shallower water toward the canyon head where oscillatory currents associated with surface waves enhance the bottom stress.

Sediment traps in the head of Lydonia Canyon trapped 2 to 3 times more material during winter when storms were frequent than during the tranquil summer. In addition, the concentration of barium, a major component of the drilling mud discharged on Georges Bank, increased in the near-bottom sediment traps deployed in the head of the canyon (station LCB, fig. 2) during the last deployment of the traps from July to November 1982. This period included the period of drilling at block 357 and block 273 (fig. 2a), both near Lydonia

Canyon. In addition, a major storm in October 1982 caused heavy sediment resuspension on the shelf which may have contributed to the transport from shelf to canyon. These observations are direct evidence of transport of sediment from the shelf to the canyon head on time scales less than one year.

Other Canyons

Near-bottom currents measured in Oceanographer Canyon were much stronger than in Lydonia or Baltimore Canyons (Lamont Doherty Geological Observatory, 1983). For example, at about 600 m in the axis, currents 5 mab exceeded 40 cm/s about 23 percent of the time in Oceanographer Canyon, but only about 10 percent of the time in Lydonia (fig. 14). Sediment traps at comparable depths along the canyon axis trapped about 1.3 times more material in Oceanographer than Lydonia. In Oceanographer Canyon, the sediments along the axis are medium to coarse sand, and there are sand waves or dunes as high as 3 m having wavelengths up to 15 m along the axis from the head to at least 600 m (Valentine and others, 1984). In contrast, the sediments along the axis of Lydonia are primarily fine and very fine sand, and large bedforms are observed only in a limited region at about 600 m. The large dunes in Oceanographer were observed to be asymmetrical down-canyon at about 250 and 600 m water depth and asymmetrical up-canyon at about 270 and 350 m. These directions are consistent with the observed net down-canyon Eulerian flow at 227 m and 560 m in Oceanographer, but also suggest cells of net up-canyon and down-canyon flow along the axis.

Based on these observations, it is clear that the major canyons along the southern flank of Georges Bank differ in size, shape, and sedimentary environment. Some of the canyons may trap fine material near their heads

while in others, the currents are strong enough to winnow and remove all fine material. Additional surveys of the sediment texture and hydrography are required to determine the sedimentary environments of other canyons.

Currents on the slope

The near-bottom observations show that the current speed decreases with depth across the slope. Below about 500 m, currents strong enough to resuspend the sediments occur only a few percent of the time, and current speeds weak enough to allow particles to settle occur more than 30 percent of the time. Particles reaching the seafloor at depths greater than 500 m will probably remain there.

The net flow over the slope is generally parallel to the isobaths at 1-10 cm/sec. Low-frequency fluctuations, also oriented along isobaths, are about 10-20 cm/s. Fine particles introduced near the surface take days to settle, and will be dispersed over wide areas before reaching the seafloor. Near the bottom, the strongest flows occur in the downslope direction and there is a persistent net downslope flow, both of which cause off-shelf and downslope transport of sediment near the bottom.

Instrument calibrations

Beam transmissometers were used extensively in the Canyon and Slope Experiments to indicate the concentration of suspended particles in the water column. Laboratory calibrations show that the sensitivity of transmissometers depends on the size of the particles in the water column as well as concentration. Thus, in situations where the size as well as the number of particles change with time, it is extremely difficult to accurately determine the magnitude of the change in suspended concentration for observed changes in

light transmission. Additional methods for determining particle size and concentration as a function of time are needed.

Sediment traps were used to estimate the vertical flux of material through the water column and to characterize the type of material in suspension. Based on a field comparison, traps of different size and shape collected material at different rates. The relative catch rates differed by as much as a factor of 5 between the traps used in this experiment and there is no way to determine which trap, if any, most closely measures the true flux of particles to the seafloor. Catch rates obtained from traps that have different hydrodynamic characteristics cannot be compared directly. Sediment traps must be calibrated in the laboratory for the current speeds and particle sizes which occur in the field.

MAJOR FINDINGS

The measurements made in the Lydonia Canyon Experiment and the Slope Experiment show:

1. Sediments from the shelf are transported into the head of Lydonia Canyon and accumulate there. These fine-grained sediments are frequently resuspended. Based on elevated inventories of ^{210}Pb and $^{239, 240}\text{Pu}$, the sediments in Lydonia Canyon scavenge pollutants from the water column. Thus the head of Lydonia Canyon is a sink for fine sediments and a potential sink for pollutants introduced onto the shelf.
2. The concentration of barium, a major component of drill muds used during exploratory drilling on the south flank of Georges Bank, increased in the head of Lydonia Canyon during the period when exploratory wells were drilled near the canyon on the shelf. This is direct evidence for transport of shelf material into the canyon.

3. The sedimentary and hydrographic regime in the major canyons on the southern flank of Georges Bank are not the same. In Oceanographer Canyon, the surficial sediments along the axis are coarser than in Lydonia and the currents are stronger. Little fine-grained sediment accumulates in the head of Oceanographer Canyon.
4. The current flow pattern within the canyon is complex. There is evidence for down-canyon transport near the head in Lydonia, Oceanographer, and Baltimore Canyons and there is up-canyon transport in Lydonia at depths of about 500 m. Additional measurements are needed to fully resolve the spatial variability in the direction of transport along the axis and its importance in determining the accumulation of sediments along the axis floor.
5. The canyons are not tranquil. The strongest flows occur at semidiurnal tidal periods, but are not always directly coupled to the tide on the shelf. Short duration packets of fluctuations occur in the canyon, some apparently generated by the passage of Gulf Stream warm core rings.
6. Gulf Stream warm core rings strongly affect the flow along the outer edge of the shelf. There is a net eastward flow in excess of 50 cm/s associated with the strongest ring events.
7. Transport of sediment at the outer edge of the shelf is in the downslope direction. At water depths below 500 m, the currents are rarely strong enough to resuspend the existing sediments and particles reaching the seafloor should remain there.

ACKNOWLEDGEMENTS

Eiji Imamura (MMS) first proposed the canyon experiment and provided continual support and advice. Jim Lane (MMS) continued the support during the final stages of the program. Pat Mullan carefully typed the manuscript.

REFERENCES

- Beardsley, R. C., Chapman, D. C., Brink, K. H., Ramp, S. R., and Schlitz, R., 1985, The Nantucket Shoals Flux Experiment (NSFE79). Part I: A basic description of the current and temperature variability: *Journal of Physical Oceanography*, v. 15, p. 713-748.
- Bothner, M. H., Rendigs, R. R., Campbell, E., Doughten, M., Parmenter, C., O'Dell, C. H., DeLisio, G. P., Johnson, R. G., Gillison, J. R., and Rait, N., 1985, The Georges Bank Monitoring Program: analysis of trace metals in bottom sediments: USGS Final Report to the U.S. Bureau of Land Management, 99 p. (prepared under Interagency Agreement 14-12-0001-30153).
- Bothner, M. H., Gilbert, J. R., and Bankstrom, D. C., Trace metals, Chapter 16 in Backus, R. H. (ed.), *Georges Bank*: Cambridge, MA, MIT Press, in press.
- Butman, B., Processes causing surficial sediment movement, chapter 13 in Backus, R.H., (ed.), *Georges Bank*: Cambridge, Mass., MIT Press (in press).
- Butman, B., and Moody, J.M., 1984, Bathymetric map of Lydonia Canyon, U.S. Atlantic Outer Continental Shelf: U.S. Geological Survey Miscellaneous Field Studies Map MF-1710, 3 plates.
- Butman, B., and Folger, D.W., 1979, An instrument system for long-term sediment transport studies on the continental shelf: *Journal of Geophysical Research*, v. 84, p. 1215-1220.
- Carson, B., Baker, E.T., Hickey, B.M., Nittrouer, C.A., Demaster, D.J., Thorbjarnarson, K.W., and Synder, G.W., 1986, Modern sediment dispersal and accumulation in Quinault Submarine Canyon - A summary: *Marine Geology*, v. 71, p. 1-13.
- Csanady, G.T., Churchill, J.H., and Butman, B., Near-bottom currents over the continental slope in the mid-Atlantic Bight: *Continental Shelf Research* (submitted).

- Danenberger, E. P., 1983, Georges Bank Exploratory Drilling (1981-1982): U.S. Department of Interior, Minerals Management Service, 20 pp.
- Farrington, J. W., and Boehm, P. D., Natural and pollutant organic compounds, Chapter 19 in Backus, R. H. (ed.), Georges Bank: Cambridge, MA, MIT Press, in press.
- Grant, W. D., and Madsen, O. S., 1979, Combined wave and current interaction with a rough bottom: Journal of Geophysical Research, v. 84, p. 1797-1808.
- Grant, W. D., and Glenn, S. M., 1983, A continental shelf bottom boundary layer model, Vol. 1: Theoretical Development: Technical Report to the American Gas Association, 167 p.
- Huggett, R. J., Nichols, M. M., and Bender, M. E., 1980, Kepone contamination of the James River Estuary: Chapter 2 in Baker, R. A. (ed.), Contaminants and sediments, Volume 1, Fate, transport, case studies, modeling, toxicity: Ann Arbor, MI, Ann Arbor Science, p. 33-57.
- Halliwell, G. R. Jr., and Mooers, C. N. K., 1979, The space-time structure and variability of the shelf water-slope water and Gulf Stream surface temperature fronts and associated warm-core eddies: Journal of Geophysical Research, v. 84, p. 7707-7725.
- Hathaway, J. C., 1971, Data File, Continental Margin Program, Atlantic coast of the United States: Woods Hole Oceanographic Institution Reference 71-15, 496 p.
- Lai, D. Y. and Richardson, P. L., 1977, Distribution and movement of Gulf Stream rings: Journal of Physical Oceanography, v. 7, p. 670-683.
- Lamont Doherty Geological Observatory, 1983, Canyon and Slope Processes Study, Volume I, Executive Summary, Final report to U.S. Minerals Management Service: Palisades, N.Y., LDGO, 12 p., (prepared under contract 14-12-0001-29178).

- Maciolek, N., Hecker, B., Butman, C., Grassle, J., Dade, W., Boehm, P., Steinhauser, W., Starczk, V., Baptiste, E., Ruff, R., and Brown, B., 1986, Study of Biological Processes on the U.S. North Atlantic Slope and Rise: Interim Report to the U.S. Minerals Management Service, 201 p. (prepared under Contract No. 14-12-0001-30064).
- Morel, F. M. M., and Schiff, S. L., 1983, Geochemistry of municipal waste in the ocean, Chapter 6 in Myers, E. P. and Harding, E. T. (eds.), Ocean disposal of municipal wastewater: impacts on the coastal environment: Cambridge, MA, MIT Sea Grant, p. 249-422.
- Richardson, P. L., 1983, in Robinson, A. R. (ed.), Eddies in Marine Science: Springer-Verlag, p. 19-64.
- Scanlon, K.M., 1984, The continental slope off New England: A long-range sidescan-sonar perspective: Geo-Marine Letters, v. 4, p. 1-4.
- Twichell, D. C., 1983, Geology of the head of Lydonia Canyon, U.S. Atlantic Outer Continental Shelf: Marine Geology, v. 54, p. 91-108.
- Valentine, P. C., Cooper, R. A., Uzman, J. R., 1984, Submarine sand dunes and sedimentary environments in Oceanographer Canyon: Journal of Sedimentary Petrology, v. 54, p. 704-715.